National Aeronautics and Space Administration

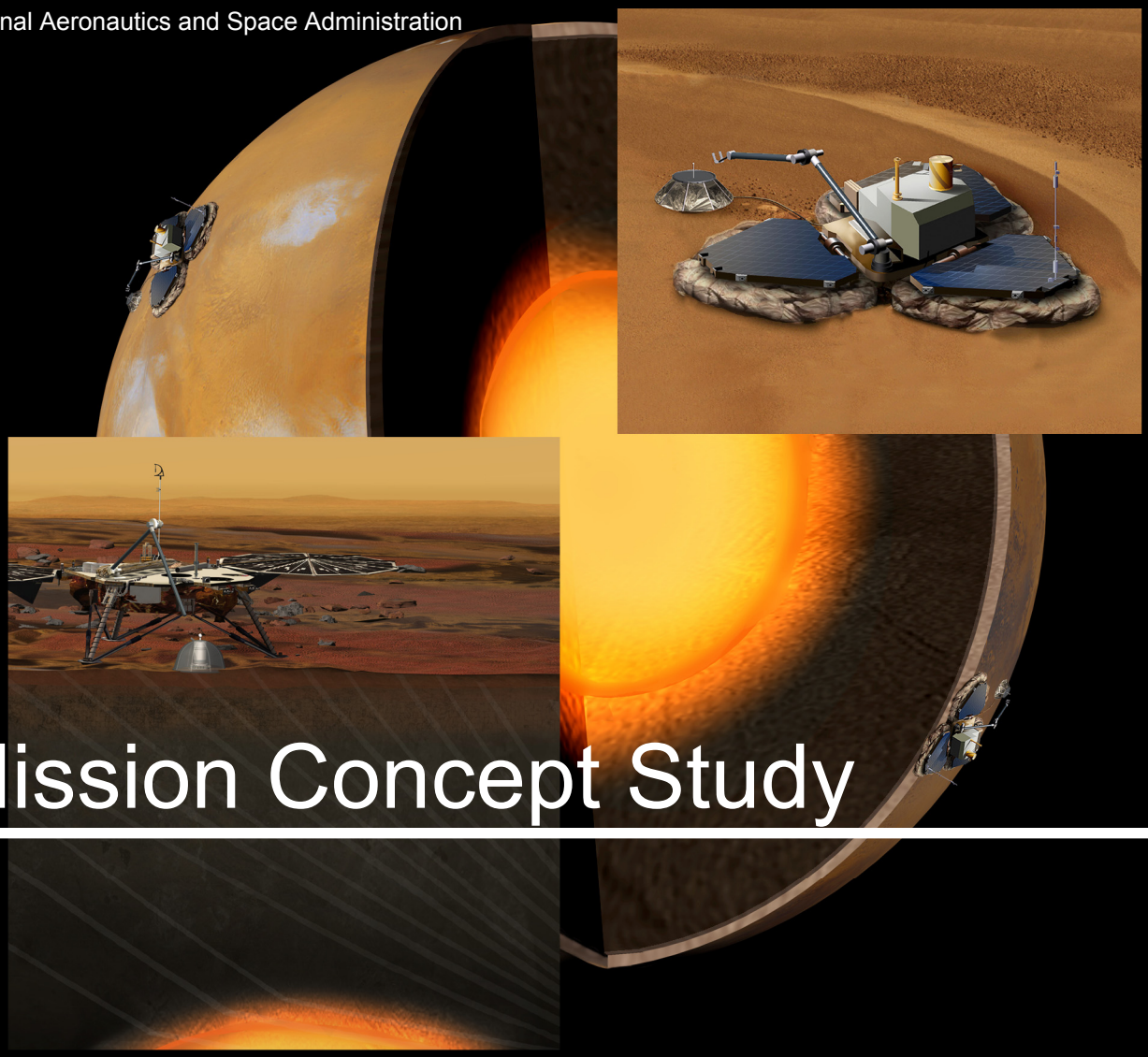

Mission Concept Study

Planetary Science Decadal Survey
Mars Geophysical Network Options

Science Champion: Dr. Lindy Elkins-Tanton (ltelkins@mit.edu)
NASA HQ POC: Lisa May (lisa.may@nasa.gov)

www.nasa.gov

July 2010

Data Release, Distribution, and Cost Interpretation Statements

This document is intended to support the SS2012 Planetary Science Decadal Survey.

The data contained in this document may not be modified in any way.

Cost estimates described or summarized in this document were generated as part of a preliminary, first-order cost class identification as part of an early trade space study, are based on JPL-internal parametric cost modeling, assume a JPL in-house build, and do not constitute a commitment on the part of JPL or Caltech. Costs are rough order of magnitude based on architectural-level input and parametric modeling and should be used for relative comparison purposes only. These costs are not validated for budgetary planning purposes.

Cost reserves for development and operations were included as prescribed by the NASA ground rules for the Planetary Science Decadal Survey. Unadjusted estimate totals and cost reserve allocations would be revised as needed in future more-detailed studies as appropriate for the specific cost-risks for a given mission concept.

Planetary Science Decadal Survey

Mission Concept Study Final Report

Figures

Tables

Appendices

A. Acronyms

B. References

Study Participants

Role	Participant	Affiliation
Study Lead	Eric Klein	Jet Propulsion Laboratory
Mars Panel Advocate Team		
Science Champion	Lindy Elkins-Tanton	Massachusetts Institute of Technology
Science	Philippe Lognonné	Institut de Physique du Globe de Paris
Technical /Management	Glenn Cunningham	Consultant
Science	Wendy Calvin	University of Nevada, Reno
JPL Study Team		
Science	Bruce Banerdt	Jet Propulsion Laboratory
Systems Engineer	Joan Ervin	Jet Propulsion Laboratory
Instruments	Kenneth Hurst	Jet Propulsion Laboratory
Mission Design / EDL	Evgeniy Sklyanskiy	Jet Propulsion Laboratory
Systems Engineer	Greg Wilson	Jet Propulsion Laboratory
Systems Engineer	Robert Shotwell	Jet Propulsion Laboratory
Systems Engineer	Keith Warfield	Jet Propulsion Laboratory
JPL SS 2012 PSDS Lead	Kim Reh	Jet Propulsion Laboratory
NASA HQ POC	Lisa May	National Aeronautics and Space Administration

Acknowledgments

This research was carried out at the Jet Propulsion Laboratory, California Institute of Technology, under a contract with the National Aeronautics and Space Administration.

Executive Summary

Several trade study sessions were conducted to survey a wide range of mission architectures that could meet, to varying degrees, the National Research Council (NRC) Mars Science Panel's proposed science objectives of a Mars Geophysical Network (MGN) mission. Nine architectures in total were investigated, five of which were targeted at New Frontiers class missions. Two Discovery class missions and two Missions of Opportunity (MOOs) were also considered. The architectures considered varied in the size of networks deployed, from one to three stations. Three different entry, descent, and landing (EDL) architectures were considered—powered descent, airbags, and rough landers. Three different cruise architectures were also assessed—one in which each lander would cruise from Earth to Mars independently (free flyers), another in which three landers would be carried together by a single cruise stage, and lastly, a secondary payload architecture in which a lander would be carried as part of another mission's payload, in the case of the MOO options.

The primary focus of the trade study was to assess the likely total project cost of each of these nine mission architectures. To that end, technical definition of each concept was pursued only to the level of detail that allowed the mission concept to be roughly modeled in the Jet Propulsion Laboratory (JPL) Advanced Project Design Team (Team X) environment, from which the cost estimates were generated. Though Team X design sessions were not held to converge on point designs for each option, previously generated Team X cost estimates for similar Mars network missions were leveraged to produce cost estimates for each option in the trade space.

Two sets of science instruments were identified that could meet the proposed science objectives of an MGN mission. The baseline payload was identified based on the measurements that would be required to meet the proposed science floor objectives, which are seismology and precision tracking. The other set included additional instruments that would significantly enhance the science return of the mission by adding heat flow, electromagnetic sounding, and boundary layer meteorology. For simplicity in comparison of costs across the trade space, all landers considered in the trade study assume just the baseline payload, and surface operations for one Mars year. Other instruments that would be carried in support of each seismometer include a robotic arm (with supporting engineering cameras) and an atmospheric instrument suite. The arm would place the seismometer on the surface at the start of science operations. After that, the arm would not be used. Cameras would be located on the arm and fixed on the deck to aid with deployment of the seismometer from the deck to the ground. The atmospheric instrument suite would be used to help understand the noise in the seismometer data, some of which originates from interaction of the atmospheric temperature, pressure, and wind with the ground or the instrument.

High-level qualitative assessments of the pros and cons of each EDL approach were briefly discussed. Rough lander concepts were quickly eliminated from the trade space due to risks associated with required technology development. From a risk perspective, neither the powered descent lander architecture nor the airbag lander architecture were seen to offer a significant advantage over each other. Some architectures were thought to be better suited to one EDL approach over another, but these advantages were marginal. Similar assessments and comparisons were made of the three cruise architectures considered.

The cost estimates generated in this study indicate that the two free-flying, powered-descent lander architecture should be feasible within the expected cost cap of a New Frontiers class mission. Similarly, the single powered-descent lander option could be feasible within the expected cost cap of a Discovery class mission.

1. Scientific Objectives

Science Questions and Objectives

Science Questions

The Mars Geophysical Network (MGN) would be a lander mission with geophysical instrumentation to study the interior of Mars. Investigations would allow, for the first time, detailed characterization of the interior of a terrestrial planet other than Earth. This would yield invaluable information about the early processes that formed the planets and subsequently shaped their surfaces and provide crucial insight into the evolution of habitability on Mars.

Our fundamental understanding of the interior of Earth comes from geophysics, geochemistry, and petrology. For geophysics, surface heat flow, magnetic, paleomagnetic, and gravity field measurements, electromagnetic (EM) techniques and, particularly, seismology have revealed the basic internal layering of Earth, its thermal structure and its gross compositional stratification, and significant lateral variations in these quantities. Understanding how life developed and evolved on Earth requires knowledge of Earth's thermal and volatile evolution and how mantle and crustal heat transfer and volatile release affected habitability at and near the planet's surface.

Mars' evolution is in sharp contrast to that of Earth. Earth's thermal engine has transferred heat to the surface largely by lithospheric recycling (plate tectonics) over much of its history; there is little evidence that this process ever occurred on Mars. The signature of early planetary processes may be preserved in Mars' internal structure, making it a particularly desirable candidate for geophysical investigation. Although Earth has lost the structures caused by differentiation and early evolution because of vigorous mantle convection, Mars may retain evidence, such as azimuthal and radial compositional differentiation in the mantle. Furthermore, much of the martian crust dates back to the first half billion years of the solar system [1]. Measurements of the planetary interior may therefore detect structures created during differentiation and early evolution, making Mars an ideal subject for understanding planetary accretion and early evolution.

Planetary interiors not only record evidence of conditions of planetary accretion and differentiation, they exert significant control on surface environments. The structure of a planet's interior and its dynamics control heat transfer within a planet through advected mantle material, heat conducted through the lithosphere, and volcanism. Volcanism in particular controls the timing of volatile release and influences the availability of water and carbon. The existence and strength of any planetary magnetic field depends in part on the size and state of the core.

The crust of a planet is generally thought to form initially through fractionation of an early magma ocean, with later addition through partial melting of the mantle and resulting volcanism. Thus, the volume (thickness) and structure of the crust can place constraints on the evolution of the putative martian magma ocean and, by extension, planetary magma oceans in general. Currently, the volume of Mars' crust is unknown to within a factor of two.

Knowledge of the state of Mars' core and its size is important for understanding the planet's evolution. The thermal evolution of a terrestrial planet can be deduced from the dynamics of its mantle and core. The state of the core depends on the percentage of light elements in the core and on the core temperature, which is related to the heat transport in the mantle [2-5]. Thus, the present size and state of the core have important implications for understanding the evolution and present state of Mars [2, 6-10].

Mantle dynamics are essential in shaping the geology of the surface through volcanism and tectonics [10]. The radius of the core has implications for possible mantle convection scenarios and in particular for the presence of a perovskite phase transition at the bottom of the mantle, which enables global plume-like features to exist and persist over time [11].

A geophysical reconnaissance of Mars should reveal at a minimum the basic radial compositional structure: the crust, the upper and lower mantle, and the solid and/or liquid core. Considerable value would also derive from placing strong constraints on the radial thermal structure. The compositional structure relates to the bulk composition of the planet and early differentiation and fractionation of the interior. Thermal structure is derived from the radial seismic velocity structure (particularly, phase boundaries), supplemented by heat flow measurements and EM sounding, and provides the “end condition” on thermal evolution scenarios. To gain full appreciation of heat transfer processes, lateral variations in mantle thermal structure must be derived from a geophysical network with an adequate distribution of stations. Strong thermal anomalies very likely remain in the mantle and the lithosphere very likely varies in thickness from hot spot processes; in fact, without this lateral information, the average radial geophysical properties may not be well determined.

The four primary methods for geophysically probing a planet’s interior from its surface are seismology, precision tracking (for rotation measurements), heat flow, and EM sounding. Each of these methods is discussed in more detail below.

Prioritized Science Objectives

The Mars Science Panel proposed science objectives for the MGN concept that would address the questions described above. These objectives are prioritized as follows:

1. Characterize the internal structure of Mars to better understand its early planetary history and internal processes affecting its surface and habitability.
    a. Characterize crustal structure and thickness.
    b. Investigate mantle compositional structure and phase transitions.
    c. Characterize core size, density, state and structure.
2. Characterize the thermal state of Mars to better understand its early planetary history and internal processes affecting the surface and habitability.
    a. Measure crustal heat flow.
    b. Characterize thermal profile with depth.
3. Characterize the local meteorology and provide ground truth for orbital climate measurements.
    a. Measure the properties related to atmospheric thermodynamics and motion

Objective 1 is considered the minimum science floor to justify MGN, with objectives 2 and 3 considered secondary.

Measurements

The best understanding of the interior of Mars would come from the synergistic analysis of many different geophysical data sets. Seismology, precision tracking, heat flow, and EM sounding have been identified by several working groups as the key measurement techniques. However, seismology is acknowledged to be by far the most valuable and effective of the methods to understand the interior of Mars. Even in the absence of complementary information on thermal state and resistivity, major advances in knowledge would be achieved by seismic measurements alone. In addition to the interior science objectives, it is recognized that meteorological measurements are particularly well served by simultaneous measurements at multiple locations on the surface. Thus, characterization of local weather processes is included as a secondary objective.

Therefore, seismology and precision tracking, which would not require additional hardware beyond the spacecraft telecommunication system, are considered the baseline payload for all of the options considered in the MGN mission concept trade study. Though EM sounding, heat flow, and more sophisticated atmospheric instruments are not included in any of the options considered, the capabilities and requirements of each of these investigations are described below. The trade study initially considered geophysical networks with one to four stations. Based on the trade study team’s assessment of science

value versus cost class, the minimum Discovery class mission would require just one station, while the minimum New Frontiers class mission would require at least two stations. The four-station missions were eliminated from the trade space early in the trade study, due to the strong evidence that no such architectures could fit within the cost constraints of a New Frontiers class mission.

Seismology

The degree of martian seismic activity remains unknown because of the high sensitivity to wind and poor installation of the Viking seismometer [12,13]. However, from models of the thermoelastic cooling of the lithosphere and extrapolation from visible faults [14-16], seismic activity approximately 100 times higher than that on the Moon has been estimated. Such a model [15] predicts approximately 100 quakes per year with seismic moment greater than 10^{14} Nm (magnitude $M_w = 3.3$) and one per year of seismic moment greater than 10^{17} Nm ($M_w = 5.3$). Impacts provide additional seismic sources and are estimated to occur at a rate similar to that of the Moon [17]. Together with estimates of seismic properties of Mars, which have been studied extensively in the last two decades [18-22], strong and conservative constraints can be used for estimating the amplitude of seismic waves. This leads to well-defined sensitivity requirements for seismic instrumentation needed to characterize the signals from a sufficient number of events and produce enough seismic data for useful analysis (see Table 1-1).

In order to fully reach the science goals described above, seismic investigations would require a network of at least four stations: three with a spacing of approximately 3,000 km (i.e., 50°) and an antipodal station capable of detecting seismic waves traveling though the core from an event simultaneously detected by the others. Such a network could provide, through P-wave travel-time analysis, confident locations for more than 80 quakes per (Earth) year and would be robust to unexpected high mantle attenuation or low seismic activity. With four or more landers, fine details of the internal structure, such as the dichotomy or other large unit differences, mantle discontinuities, and anisotropy, might also be characterized.

Although a network of four or more stations would be ideal, fewer stations could still provide much of the necessary information for addressing the science objectives described above. There are many analysis techniques that have been developed for seismology, particularly in the last decade that could extract interior information from seismic measurements at fewer stations, or even a single station. One seismic station could use techniques such as P-S/back-azimuth tracing to provide locations, multiple phase arrivals (P, S, PmP, PcP, PKP, etc.) to derive interior velocities and boundary depths, receiver function and surface wave analysis to delineate crust and upper mantle structure, and Phobos tide measurements and possibly normal mode observations to constrain core size and state. Two stations constitute a substantial improvement in capability, providing correlation capacity for unambiguous identification of seismic events, an improved ability to compute surface wave phase velocity, and noise correlation techniques that can provide planetary structure from background noise analysis while strengthening the interpretation of the single-station techniques described above. A three-station network has the additional advantage that it could provide event locations using conventional P-wave arrival techniques combined with a limited set of a priori assumptions.

For this study a two-station network of seismometers is considered the minimum network size to address the baseline science of MGN for a New Frontiers class mission. However, single station missions were also investigated, as they would provide science value commensurate with Discovery class missions.

Precision Tracking—Geodesy

Precision tracking of the martian surface would be performed through radio links between ground stations on Earth and landers on the surface of Mars. The experiment would consist of an X-band (or Ka-band) transponder designed to obtain two-way Doppler and/or ranging measurements from the radiometric link. These Doppler measurements, taken over a long period of time (at least one martian year), could be used to obtain Mars' rotation behavior (i.e., precession, nutations, and length-of-day variations). The ultimate objectives of this experiment would be to obtain information on Mars' interior and on the mass redistribution of CO_2 in Mars' atmosphere. Precession (long-term secular changes in the rotational orientation) and nutations (periodic changes in the rotational orientation) as well as polar motion (motion of the planet with respect to its rotation axis) would be determined from this experiment and used to obtain information about Mars' interior. At the same time, measurement of variations in Mars' rotation rate

could determine variations of the angular momentum due to seasonal mass transfer between the atmosphere and ice caps [23-35].

Precession determination would improve the determination of the moment of inertia of the whole planet and the radius of the core. For a specific interior composition or even for a range of possible compositions, the core radius is expected to be determined with a precision of a few tens of kilometers. A precise measurement of variations in the orientation of Mars' spin axis would also enable, in addition to the determination of the moment of inertia of the core, an even better determination of the size of the core via the core resonance in the nutation amplitudes. A large inner core can also have an effect on the nutations that could be measured by radio tracking due to the existence of resonance in the free inner core nutation.

A great deal has already been learned from such experiments on Viking and Mars Pathfinder (MPF), but better accuracy than Viking (≤0.1 mm/s) and a longer time span than MPF (which lasted ~60 sols) are necessary for significant advances.

Enhancement Options: Heat Flow, Electromagnetic Sounding, and Boundary Layer Meteorology

Heat Flow: Planetary heat flow is a fundamental parameter characterizing the thermal state of a planet. Knowledge of the present-day heat flux on Mars would elucidate the workings of the planetary heat engine and provide essential boundary conditions for models of the martian thermal evolution. This would enable us to discriminate between different evolution models, all of which have different predictions for when the dynamo was active. A determination of the average heat flow would also provide important constraints on the abundance of radioactive isotopes in the martian interior, which in turn would place limits on the major element chemistry. By measuring the mantle contribution to the heat flow in regions of thin crust (e.g., the Hellas basin), questions concerning the distribution of heat-producing elements between crust and mantle and the process of planetary differentiation could also be addressed.

Planetary heat flow determines the depth at which liquid water is stable below the surface and thus directly bears on this critical habitability parameter [36]. Furthermore, geothermal energy (i.e., heat flow) is the most important energy source in the martian subsurface today and knowledge of the planetary heat flow would directly constrain the potential for biological activity on present-day Mars.

To measure heat flow, the thermal conductivity and thermal gradient in the regolith need to be determined. This would be achieved by emplacing temperature sensors and heaters in the subsurface. Thermal conductivity would then be determined by active heating experiments or an analysis of the decay of the annual temperature wave. Measurement uncertainties for the thermal conductivity and thermal gradient measurements should be below 10% each, resulting in an uncertainty of 15% for the heat flow. To achieve this accuracy, temperature sensors would need to be calibrated to within 0.1 degree K.

The heat flow from the interior is expected to be similar in large provinces on the martian surface. The measurement sites should ideally include a representative highland and lowland site, a measurement in the volcanically active Tharsis province, and a determination of the mantle heat flow from a measurement in the Hellas basin. However, even a single measurement would be an extremely valuable addition to our knowledge of Mars.

Electromagnetic Sounding: Electromagnetic sounding has yielded important insights on the interior structures of the Moon and the Galilean satellites [37-39]. EM methods are widely used to understand Earth's structure from depths of meters to hundreds of kilometers. Proposed objectives for Mars include the temperature and state of the upper mantle, the thicknesses of the lithosphere, crust, and cryosphere, and lateral heterogeneity in any of these properties. EM measurements are therefore complementary to seismology and heat flow in constraining the internal structure and evolution of Mars.

Time-varying EM fields induce eddy currents in planetary interiors, whose secondary EM fields are detected at or above the surface. These secondary fields shield the deeper interior according to the skin-depth effect, so that EM fields fall to 1/e amplitude over depth δ (km) = $0.5\sqrt{\rho}/f$, where ρ is the resistivity (in Ω-m) and f is the frequency (in Hz). EM sounding exploits the skin-depth effect by using measurements over a range of frequency to reconstruct resistivity over a range of depth [40]. Natural EM signals (i.e., magnetospheric pulsations, ionospheric currents, lightning) are used instead of transmitters

at the low frequencies necessary to penetrate kilometers to hundreds of kilometers into the Earth. Sources for Mars would likely include direct solar-wind/ionosphere interactions, diurnal heating of the ionosphere, solar-wind/mini-magnetosphere interactions, and possibly lightning. These sources would provide a spectrum from ~10 μHz (1 sol period) to >1 kHz.

Forward modeling of a variety of possible subsurface structures for Mars provides a broad mapping of measured frequency to depth of investigation. The cryosphere, from the surface to a depth of a few to tens of kilometers, is probably very resistive and hence EM-transparent. Underlying saline groundwater would be a near-ideal EM target. Grimm [41] shows that the depth to groundwater could be determined from measurements anywhere in the range of 1 mHz to 1 kHz. A wet crust would partly shield the deeper interior on Mars as on Earth, but, in both cases, frequencies of 1–100 μHz penetrate and are sensitive to hundreds of kilometers depth. Higher frequencies (up to 100 mHz) penetrate to these depths if the crust is dry. There appears to be a good match, therefore, between the likely natural EM energy and the necessary investigation depths for the EM science objectives.

The fundamental quantity that must be derived is the frequency-dependent EM impedance *Z*. Two methods are suitable for constructing *Z* from measurements at the surface of Mars. Geomagnetic depth sounding uses surface arrays of magnetometers to determine *Z* from the ratio of the vertical magnetic field to the magnitude of the horizontal magnetic-field gradient [42]. Using this method, frequencies 10–100 μHz from ionospheric sources could be used to probe the mantle. The magnetotelluric method (MT) uses orthogonal horizontal components of the local electric and magnetic fields to compute *Z*. Mars MT would likely best apply to higher frequencies (<1 Hz to ~1 kHz) and hence exploit 0.01–1 Hz direct solar-wind/ionosphere interactions [43] as well as Schumann resonances (~10–50 Hz) and TM waves (>100 Hz) due to lightning. MT would therefore focus on the crust and cryosphere. Together, geomagnetic depth sounding and MT would address the proposed MGN mission science goals.

Boundary Layer Meteorology: Although meteorological payloads on an interior-focused, two-lander network mission could not fully address the global measurements required to meet the highest priority Mars Exploration Program Advisory Group (MEPAG) climate goals and investigations [44], they could address important elements of the goal related to the dust, H_2O, and CO_2 cycles, as well as the behavior of trace gases that are exchanged with the surface. Specifically, a two-lander network mission could characterize the nature of surface-atmosphere interactions and how they vary in space and time. These interactions could only be determined from surface measurements rather than orbiters and have yet to be adequately characterized by any previous landed mission. The most important aspect of these interactions is the exchange of heat, momentum, water vapor, and trace species between the surface and atmosphere. Understanding these exchanges requires long-term, carefully calibrated, and systematic measurements of pressure, temperature, 3D winds, dust, water vapor, solar and infrared energy inputs, and the electrical environment. Such measurements, made at sufficiently high cadence and with some vertical discrimination, would yield quantitative estimates of the vertical turbulent fluxes of heat, mass, and momentum, which in turn would determine the surface forcing of the general circulation and the sources and sinks for dust, H_2O, and CO_2. Depending on how the network is configured, correlation studies could further help characterize the near surface signature of regional and larger-scale weather systems such as slope flows, baroclinic eddies, and thermal tides, especially if further supplemented with contemporaneous measurements from orbit.

Science Traceability

Table 1-1. Science Traceability Matrix

Science Objective	Measurement	Instrument	Functional Requirement
Characterize the internal structure of Mars to better understand its early planetary history and internal processes affecting its surface and habitability	Characterize crustal structure and thickness Investigate mantle compositional structure and phase transitions Characterize core size, density, state, and structure	VBB seismometer	• At least one Mars year of continuous measurements • 3-axis; noise floor better than 0.5×10^{-9} m/s^2/Hz$^{1/2}$ from 2 mHz–5 Hz
		X-band transponder	• At least one Mars year of weekly measurements • 0.1 mm/s for 60 s integration
		EM sounder (passive)	• 3-axis magnetometer: 0.01 nT/Hz$^{1/2}$ from 1 mHz–5 Hz; 0.1 nT DC • 2-axis electrometer: 0.1 mV/m/Hz$^{1/2}$, 1 mHz–5 Hz
Characterize the thermal state of Mars to better understand its early planetary history and internal processes affecting the surface and habitability	Measure crustal heat flow	Mole with instrumented tether	• At least one Mars year of daily measurements • Temperature: 0.1 K relative precision at ≥10 points to 3 m depth • Thermal conductivity: 10%
	Characterize thermal profile with depth	EM sounder (passive)	• As above
Characterize the local meteorology and provide ground truth for orbital climate measurements	Measure the properties related to atmospheric thermodynamics and motion	Pressure sensor	• 1–3 Pa accuracy at rates to 3 Hz
		Thermistors	• 0.01 K accuracy at rates to 1 Hz over a range of height to >1 m
		Hot-wire anemometer	• 2D speed and direction • 10% accuracy from 0.1–100 m/s at rates to 1 Hz
		Acoustic anemometer	• 3D speed and direction, vertical shear • 10% accuracy from 0.1–100 m/s at rates to 8 Hz
		Humidistat	• Better than ±5% accuracy at Mars ambient temperatures
		Electrometer	• Quasi-DC E field from 10 V/m–10 kV/m • AC field from 10 Hz–4 kHz with a sensitivity of 2 μV/m

Note: This matrix describes the linkages between science objectives and how they would be achieved. Blue shading indicates the proposed science floor objectives, measurements, instruments, and associated functional requirements. Note that the pressure sensor, thermistors, and hot-wire anemometer are defined as science floor instruments because they are required for the proper calibration of the seismometer. These atmospheric instruments would also satisfy some of the proposed meteorology science objectives, but as a whole, these objectives are not part of the baseline science of MGN.

2. High-Level Mission Concept

Overview

The MGN mission architectures studied were narrowed down to two landing architectures: airbag landers and powered-descent landers. Each landing architecture assessed the impacts of varying the number of landed stations from one to three. Additionally, three different cruise architectures were considered—one in which each lander would cruise from Earth to Mars independently (free flyers), another in which three landers would be carried together by a single cruise stage (common carrier), and lastly, a secondary payload architecture in which a lander would be carried as part of another mission's payload, in the case of the MOO options. Table 2-1 and Figure 2-1 describe the nine mission options studied, their corresponding landing architecture, number of stations, cruise architecture, and the target mission class.

All mission architectures assumed in this study assume the existence of a relay orbiter at Mars that would be capable of receiving data from the landers UHF telecom system and relaying the data to Earth via either X- or Ka-band. All mission architectures are also constrained to a single launch, and assume one martian year primary science duration on the surface of Mars.

Table 2-1. Option Descriptions

Option ID	Landing Architecture	# Stations	Cruise Architecture	Target Class
A	Airbag	3	Free Flyer	New Frontiers
B	Airbag	3	Common Carrier	New Frontiers
C	Airbag	2	Free Flyer	New Frontiers
D	Powered descent	3	Free Flyer	New Frontiers
E	Powered descent	2	Free Flyer	New Frontiers
F	Powered descent	1	Secondary Payload	MOO
G	Powered descent	1	Free Flyer	Discovery
H	Airbag	1	Free Flyer	Discovery
I	Airbag	1	Secondary Payload	MOO

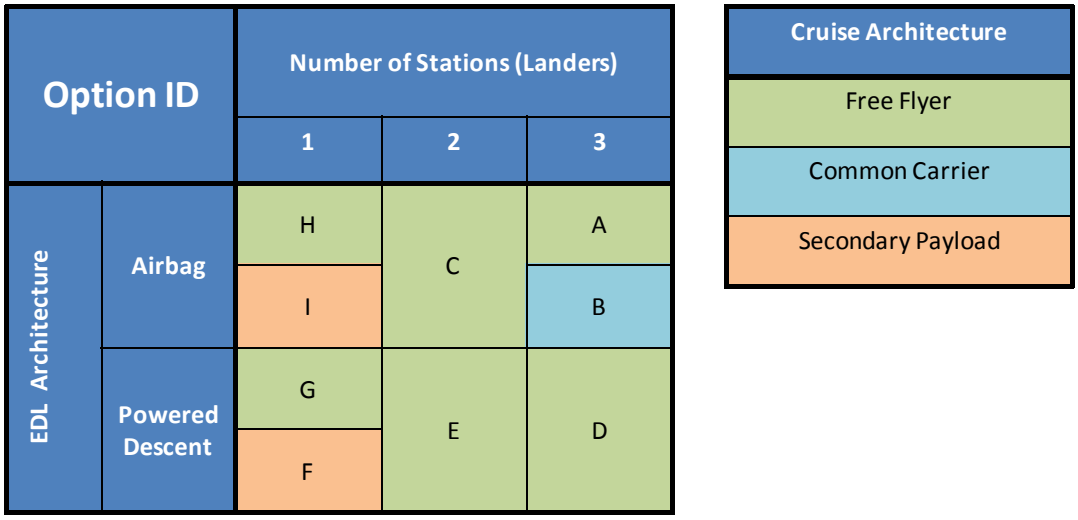

Figure 2-1. Option Descriptions

Tables 2-2 and 2-3 document the key characteristics of the different cruise and lander architectures.

Table 2-2. Key Architecture Characteristics

Phase/ System	Powered Free Flyers	Airbag Free Flyers	Airbag Common Carrier	Secondary Payload (Powered or Airbag)
Launch / Early Cruise	Stacked launch configuration releases from dispenser with 3-axis stabilization.	Stacked launch configuration releases from dispenser with spin stabilization.	Stacked launch configuration stays attached to the 3-axis stabilized “smart” dispenser.	Launch configuration dependent on specific MOO. Carried as payload.
Late Cruise	Each entry system separation from cruise stage at entry minus 15 minutes. Entry separation ~7 days. Late updates possible.	Each entry system separation from cruise stage at entry minus 15 minutes. Entry separation ~7 days. Late updates possible.	Individual entry system release starting at entry minus 15 days, entry minus 8 days, entry minus 1 day.	Node released between entry minus 10 and entry minus 2 days out. Release would occur prior to MOO Mars orbit insertion.
Detached Cruise	Use secondary battery with heaters and full power avionics.	Use secondary battery with heaters and low power timing avionics mode.	Multiple deployments off common carrier with spin eject mech. Passive thermal control, low power timing avionics mode until entry minus 1 hour. Late updates are not possible.	Lander released with spring ejection mechanism. Use secondary battery with heaters.
EDL	No spin during entry, supersonic DGB parachute.	Spinning during entry, ballistic entry, supersonic DGB parachute, no DIMES / TIRS.	Spinning during entry, ballistic entry, supersonic DGB parachute, no DIMES / TIRS.	See powered or airbag free flyer.
Terminal Descent	Liquid pulsed propulsion, legged lander.	Solid RAD rockets with MER airbag system, tetrahedron lander.	Solid RAD rockets with MER airbag system, tetrahedron lander.	See powered descent or airbag free flyer.

Table 2-3. Key Architecture Metrics

Phase/ System	Powered Free Flyers	Airbag Free Flyers	Airbag Common Carrier	Secondary Payload (Powered or Airbag)
Timing of Separation from Dispenser, Common Carrier, or Primary Element	Trans-Mars injection +2 hours	Trans-Mars injection +2 hours	Entry minus 15, entry minus 8, and entry minus 1 day	Between entry minus 10 and entry minus 2 days
Entry Type	Prograde	Prograde	Prograde	Prograde
Entry Time Phasing	7 days apart	7 days apart	1–12 hours a part	N/A (single lander)
Landing Site Altitudes	−2.8 km MOLA	0 km MOLA	See airbag free flyers	See free flyers (powered or airbag)

Phase/ System	Powered Free Flyers	Airbag Free Flyers	Airbag Common Carrier	Secondary Payload (Powered or Airbag)
Landing Ellipse	150×30 km for all	150×30 km for all	250×80, 100×20, 80×20 km	See free flyers (powered or airbag)
Entry Mass	560 kg	780 kg	See airbag free flyers	See free flyers (powered or airbag)
Maximum Entry Velocity	6.0 km/sec	6.0 km/sec	See airbag free flyers	See free flyers (powered or airbag)
Landed Mass (per station)	340 kg	502 kg	See airbag free flyers	See free flyers (powered or airbag)
Landing Velocity Magnitude	<1 m/sec	<20 m/sec	See airbag free flyers	See free flyers (powered or airbag)

Concept Maturity Level

Table 2-4 summarizes the NASA definitions for concept maturity levels (CMLs). Based on an assessment of the results of this study, this concept is considered to be at CML 3. The architecture studied was defined at the assembly level based on previous Team X studies with estimates developed for mass, power, data volume, link rate, and cost using JPL's institutionally endorsed design and cost tools. Risks were also identified and assessed as to their likelihood and mission impact, as discussed later in the report.

Table 2-4. Concept Maturity Level Definitions

Concept Maturity Level	Definition	Attributes
CML 6	Final Implementation Concept	Requirements trace and schedule to subsystem level, grassroots cost, V&V approach for key areas
CML 5	Initial Implementation Concept	Detailed science traceability, defined relationships, and dependencies: partnering, heritage, technology, key risks and mitigations, system make/buy
CML 4	Preferred Design Point	Point design to subsystem level mass, power, performance, cost, risk
CML 3	Trade Space	Architectures and objectives trade space evaluated for cost, risk, performance
CML 2	Initial Feasibility	Physics works, ballpark mass and cost
CML 1	Cocktail Napkin	Defined objectives and approaches, basic architecture concept

Technology Maturity

No technology development would be required for this mission. This is largely in keeping with the initial design goal of consistency with competitive missions. The options considered leverages flight proven technologies such as airbags, powered descent, landing radar, and robotic arm heritage from previous Mars missions including MPF, Mars Exploration Rover (MER), and Phoenix. Key technology development for the seismometer has been conducted over the past two decades, culminating in a technology readiness level (TRL) 5–6 instrument developed for the European Space Agency (ESA) ExoMars mission as part of the Humboldt package. The baseline atmospheric instruments are all high TRL and have heritage from the MPF, Mars Polar Lander (MPL), and Phoenix missions.

Key Trades

Landing Architecture: Powered Descent vs. Airbag vs. Rough Lander

The landing architectures considered in this trade study included powered descent landers similar to the Phoenix and Viking missions, airbag landers similar to the MPF and MER missions, and rough landers. The advantages of a powered descent system include the ability to utilize a single integrated propulsion system for the lander and cruise stage, lower flight system mass, larger volume (and mass) available for payload, and the ability to accommodate larger landed solar arrays. The main advantages of an airbag lander include the robustness of the landing approach and lower recurring flight system costs. The rough lander concept was only briefly considered before being removed from the trade space. Though rough landers could greatly simplify the flight system architecture, and would probably also be lower in mass and recurring cost than either the powered descent or airbag lander systems, they would require significant technology development, and would likely have an increased risk of SEIS deployment failure as compared to the powered descent and airbag systems. Because both the powered descent and airbag landing systems have flight heritage, these architectures were carried forward for additional study. With sufficient funding for technology development and risk reduction, the rough lander architecture could prove to be the most cost effective way to implement a large martian geophysical network. However, due to the fact that this trade study was constrained to competitively selected, AO-driven Discovery and New Frontiers class missions, the risk (and cost risk) associated with a new technology development program was determined to be excessive and the rough lander architectures were not carried forward for further consideration.

Cruise Stage Architecture Free Flyer vs. Common Carrier

One approach considered for a three-airbag lander architecture would be to utilize a “common carrier” that would deliver the combined entry systems/landers to Mars with a single cruise stage/carrier element. Though this architecture would eliminate the need for the three simple cruise stages and the dispenser, it would require a more complex carrier flight element that must still support the combined mass of each entry system and lander during launch, and be able to release them shortly before Mars arrival. This approach does have issues associated with achieving the desired entry separation. The most significant challenge was the entry system design required to meet the power and thermal needs of the lander during detached cruise without solar power. The addition of body-fixed solar cells to the exterior of the backshell was considered, but the additional cost and complexity were thought to outweigh the savings achieved through the elimination of the simple cruise stages. The option of relaxing the entry separation from seven days down to a few hours was also considered, but this would increase risk during EDL, possibly to unacceptably high levels. The primary concern was the stress on the mission operations system and the inability to react to anomalies encountered during the EDL sequence of the first lander. For these reasons, the common-carrier approach was not favored by the study team, but a cost estimate was generated for comparison purposes.

3. Technical Overview

Instrument Payload Description

The proposed instrument payload for each lander in each MGN mission architecture option would be identical, and would be consistent with the baseline science described in Section 2. The instruments that comprise this payload include the seismometer (SEIS), instrument deployment arm (IDA), instrument deployment camera (IDC), stereo cameras, atmospheric instrument suite (ATM), and X-band transponder. The baseline ATM is made up of temperature and pressure sensors and a hot-wire anemometer. The precision tracking experiment is also included in each MGN mission architecture option, though the hardware needed to conduct this experiment is part of each lander's telecommunications subsystem.

Secondary science instruments, such as a heat flow probe (HP^3), dust opacity and concentration instruments, an electromagnetic sounder (EMS), a humidistat, and sonic anemometer instruments are not included in any of the MGN options and are not needed to meet the baseline science objectives. However, if there were sufficient resources to include these instruments they would provide considerably enhanced science directly addressing the goals of the mission. Thus, descriptions of these optional instruments are included below. The impact on the flight system caused by the addition of the secondary science instruments has not been fully evaluated, but is expected to be minimal. For example, the Phoenix mission flew with a science payload of approximately 60 kg, but the current proposed MGN payload is only 25 kg (CBE + 30% contingency).

Table 3-1 provides the mass and power details for the baseline instrument payload.

Table 3-1. Payload Mass and Power Estimates

	Mass			Average Power		
	CBE (kg)	**% Cont.**	**MEV (kg)**	**CBE (W)**	**% Cont.**	**MEV (W)**
Seismometer	6	33%	8	1.8	33%	2.4
IDA (robotic arm)	5	40%	7	28	43%	40
IDC (Navcam)	0.22	50%	0.33	2.2	36%	3
Stereocams (2)	0.44	50%	0.66	4.4	36%	6
ATM (P,T, W)	1.5	67%	2.5	2	50%	3
Total Estimated Payload Mass	**13.2**	**40.5**	**18.5**	**38.4**	**41.7**	**54.4**

Seismometer

The seismometer described below is based on a design that has been offered by an international collaboration on numerous previous NASA mission concepts and proposals dating from the mid-90s to the present. The most current configuration of the seismometer encompasses hardware from France (Institut de Physique du Globe de Paris), the United Kingdom (Imperial College, London), Germany (Max Planck Institute, Lindau), Switzerland (Swiss Federal Institute of Technology, Zurich), and the US (Jet Propulsion Laboratory, Pasadena). The instrument relies on the ExoMars Geophysical Package (GEP) development that was based on the NetLander Phase B development, which in turn built on the foundation of the OPTIMISM experiment for the Mars'96 mission. It is the subject of continuing development for use on the Moon by the Japanese SELENE-2 mission.

This instrument was chosen for the study because it is the only design currently available that would fulfill the demanding proposed science measurement requirements and would be compatible with planetary flight and operational requirements. Although it is largely a non-US development, it has been assumed that the cost of building the hardware would be borne by NASA. The components of the instrument are

developed by various European research institutes; however, the institutes do not fabricate flight instruments, but rather contract them to industry. The estimated cost for this approach, which is the baseline assumed for the MGN mission concept, in this study is the anticipated industrial contract cost based on information supplied by the European developers.

Two other acquisition options are possible. The first would be a contribution by the European agencies responsible for the development (CNES in France, DLR in Germany, the UK Space Agency, and CFAS/PRODEX in Switzerland). There is a long-standing collaboration among European and US investigators that has led to such contributions being endorsed for many NASA proposals (and US contributions being endorsed for ESA proposals), so this option is considered quite plausible.

The second alternative would be a US-only development. It would be necessary to take a classical, terrestrial very broad band (VBB) seismometer with the required performance, decrease its mass and power, and qualify it for flight loads, radiation, and Mars surface temperature conditions. For example, a Streckeisen STS-2 is one of the few terrestrial VBB sensors with the required performance. It weighs approximately 9 kg, requires approximately 1.2 W for the sensor, and has already been operated in Antarctic conditions below –50°C. (Note however that even terrestrial seismology is a very international undertaking. Streckeisen is a Swiss company, although it is owned by Kinemetrics in the US. The US dense seismological network set up by IRIS uses exclusively European broad band sensors, either from Streckeisen of Switzerland or Guralp of the UK.) The ~10-year VBB technology development program in France has lead to a reduction of the mass by a factor of 3–4 and of the power by a factor of 2–3, while making the instrument compatible with g-loads of 200 g. It is estimated that it would take $10–15M (FY10) and approximately 4 years for a US team to develop a comparable VBB instrument based on an existing terrestrial design, perhaps with more modest mass, power, and shock resistance improvement goals. SP sensors are currently available that would require modest development for flight qualification. The acquisition electronics are also relatively standard and are comparable to the acquisition electronics of a magnetometer, for which US expertise is available.

Instrument Description: The SEIS instrument is composed of an evacuated sphere assembly, enclosing three VBB orthogonal oblique seismometers, along with three additional independent orthogonal short period (SP) seismometers outside the sphere. The sphere is thermally decoupled from the environment by an insulated wind cover. The sphere also encloses a set of secondary sensors (temperature and inclination) used for both instrument management and scientific purposes. Pressure sensors are both inside (for monitoring the vacuum quality) and outside (for monitoring atmospheric pressure changes) the sphere. The external pressure sensor is sampled at 20 Hz to cover the infrasonic range. The VBB seismometer has been under development by IPGP since the late 1980s and the SP was developed first by JPL and later by Imperial College since the mid-90s.

The seismometer noise power spectral density, which defines the noise floor of the instrument, is shown in Figure 3-1. Figure 3-2 provides the response and noise curves for the seismometer. It meets the proposed mission requirements for the VBB seismometers ($<10^{-9}$ m/s^2/Hz$^{1/2}$ from 10^{-3}–2 Hz) and the SP seismometers ($<10^{-8}$ m/s^2/Hz$^{1/2}$ from 5×10^{-2}–100 Hz). The SP seismometer is sampled at a selectable rate between 20 and 200 Hz and the VBB seismometer is sampled at a selectable rate between 2 and 20 Hz. Details of the SEIS are provided in Table 3-2.

The IDA would deploy the seismometer package from its stowed position on the lander onto the surface of Mars. A tether would provide power and data connection between the SEIS and the warm electronics module (WEM). Three fixed, pointed feet on the bottom of the seismometer would aid high frequency coupling to the martian soil. The instrument would be fully operational after its initialization sequence (i.e., leveling, pendulum centering, and feedback tuning). This sequence and the subsequent calibration activity, which consists of monitoring the temperature impact on the instrument in order to set the thermal loop compensation, would last several weeks. The SEIS instrument including the leveling mechanism was at TRL 6 and passed PDR for the ExoMars mission before being descoped. Recent changes to the system have reduced the TRL to 5; however, there is an existing funded plan to return to TRL 6 by the fall of 2010. The development is being funded by CNES, for use on the Japanese SELENE-2 mission.

Figure 3-1. SEIS showing the evacuated sphere where the VBB sensors are located, the base, and support structure.

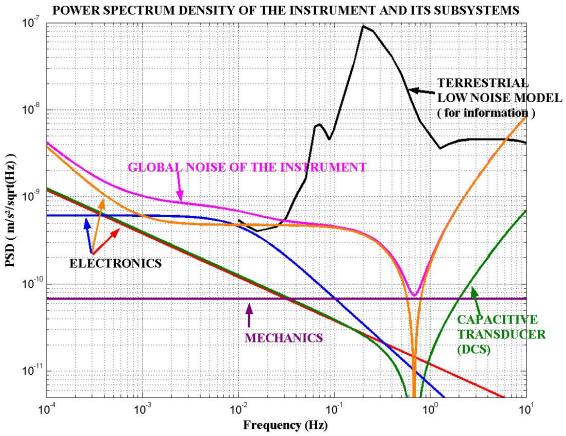

Figure 3-2. Response and noise curves for the seismometer.

Table 3-2. SEIS

Item	Value	Units
Type of instrument	Seismometer	
Number of channels	>20	
Size/dimensions (for each instrument)	0.3 h x 0.4 dia	m x m x m
Instrument mass **without** contingency (CBE*)	6	kg
Instrument mass contingency	33%	%
Instrument mass **with** contingency (CBE+Reserve)	8	kg
Instrument average power **without** contingency	1.8	W
Instrument average power contingency	33%	%
Instrument average power **with** contingency	2.4	W
Instrument average science data rate^ **without** contingency	8	kbps
Instrument average science data^ rate contingency	31%	%
Instrument average science data^ rate **with** contingency	10.5	kbps
Sensitivity	$<10^{-9}$ m/s^2 Hz$^{-1/2}$ from 10^{-3} to 10 Hz $<10^{-8}$ m/s^2/Hz$^{1/2}$ from 5×10^{-2} to 100 Hz	
Instrument fields of view (if appropriate)	N/A	degrees
Pointing requirements (knowledge)	1	degrees
Pointing requirements (control)	N/A	degrees
Pointing requirements (stability)	N/A	deg/sec

*CBE = Current best estimate

^Instrument data rate defined as science data rate prior to on-board processing

Instrument Deployment Arm

The proposed requirement for the IDA is to provide access to a range of at least 2 m and 150° on terrain slopes of up to 15° for placement of the seismometer. The IDA described here meets all proposed requirements and is a Phoenix-derived design, but with reduced link lengths and brushless motors. It would have 4 DOF (i.e., shoulder yaw and pitch, elbow and wrist pitch). Each of the four actuators would carry a temperature sensor and heater and use a potentiometer for broad position determination and a magnetoresistive relative-count encoder for precise motion determination. The IDA would carry an end-effector on the wrist joint (Figure 3-3). Based on a "crow's foot and grapple" approach, this simple design would allow for reliable instrument manipulation even with maximum IDA positioning error (5 mm close to the arm base, 2 cm when fully extended). The concept was brought to critical design review (CDR)-level during the Mars Surveyor '01 project planning phase and was tested on slopes up to 16°.

As each instrument is deployed, a cable box would passively pay out the umbilical tethers that connect the instrument to the WEM electronics and power supply. The cables would be in an accordion pleat configuration inside the boxes and would be strong, flexible, and strain relieved.

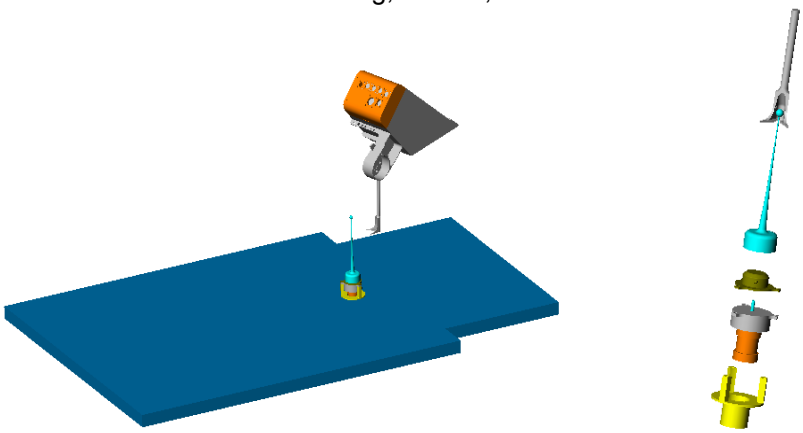

Figure 3-3. IDA end effector and ball-on-stalk device for picking up and placing SEIS on the ground.

Camera Systems

The purpose of the camera system would be to support seismometer deployment. It would consist of an IDC and a pair of Stereocams. The IDC, which has MER Navcam heritage (Figure 3-4), would be attached to the forearm of the IDA and would be used for imaging deployments. It could also be used to study the surrounding geology and perform atmospheric dust opacity measurements. Two Stereocams based on the MER Hazcams would be fixed to the lander and would provide stereo images of the work area reachable by the IDA. The IDC would be fitted with a set of filters of the same design as the Pancam in order to monitor dust opacity. Technical interface details for the cameras are provided in Tables 3-3 and 3-4.

Figure 3-4. Navcam Camera on Which the IDC Would be Based

Table 3-3. Instrument Deployment Camera

Item	Value	Units
Type of instrument	Camera	
Number of channels	1	
Size/dimensions (for each instrument)	0.04 x 0.05 x 0.02	m x m x m
Instrument mass **without** contingency (CBE*)	0.22	kg
Instrument mass contingency	50%	%
Instrument mass **with** contingency (CBE+Reserve)	0.33	kg
Instrument average power **without** contingency	2.2	W
Instrument average power contingency	36%	%
Instrument average power **with** contingency	3	W
Instrument average science data rate^ **without** contingency	2,000	kbps
Instrument average science data^ rate contingency	25%	%
Instrument average science data^ rate **with** contingency	2,500	kbps
Sensitivity	0.76	mrad/pixel
Instrument fields of view (if appropriate)	N/A	degrees
Pointing requirements (knowledge)	N/A	degrees
Pointing requirements (control)	N/A	degrees
Pointing requirements (stability)	N/A	deg/sec

*CBE = Current best estimate

^Instrument data rate defined as science data rate prior to on-board processing

Table 3-4. Stereocams (Two)

Item	Value	Units
Type of instrument	Camera	
Number of channels	1	
Size/dimensions (for each instrument)	0.04 x 0.05 x 0.02	m x m x m
Instrument mass **without** contingency (CBE*)	0.22	kg
Instrument mass contingency	50%	%
Instrument mass **with** contingency (CBE+Reserve)	0.33	kg
Instrument average power **without** contingency	2.2	W
Instrument average power contingency	36%	%
Instrument average power **with** contingency	3	W
Instrument average science data rate^ **without** contingency	2,000	kbps
Instrument average science data^ rate contingency	25%	%
Instrument average science data^ rate **with** contingency	2,500	kbps
Sensitivity	1.2	mrad/pixel
Instrument fields of view (if appropriate)	N/A	degrees
Pointing requirements (knowledge)	N/A	degrees
Pointing requirements (control)	N/A	degrees
Pointing requirements (stability)	N/A	deg/sec

*CBE = Current best estimate

^Instrument data rate defined as science data rate prior to on-board processing

X-Band Transponder

The X-band transponder would be the same hardware used by the spacecraft for communication with Earth during cruise. No data would be collected on Mars. The transponder must be on for 1 hour per week for the duration of the mission. The transponder would require 43 W of power when it is operational. It may be possible to turn off the main amplifier for much of the tracking pass and only transmit back to Earth at the beginning and end of the pass. The receiver on Mars would have to accumulate phase during the time between transmissions. If this power saving technique were used, the power requirement would drop to 19 W during the non-transmitting period.

Atmospheric Instruments

The atmospheric instruments would be mounted on a 1.2 m tall mast, which would use spring action to deploy itself to an attitude perpendicular to the lander deck when the latch is released. The instruments would consist of pressure and temperature sensors, and an anemometer. Technical details of the ATM are provided later in this section in Table 3-5.

Atmospheric Pressure

An atmospheric pressure gauge would be housed in the WEM with a 2 mm diameter port to the atmosphere. The sensor would have an absolute accuracy of 1–3 Pa throughout the range of pressures anticipated on the martian surface (500–1,200 Pa). The output would consist of a 4–12 kHz signal monitored by a 10 MHz counter, providing a resolution of ~25 mPa for an integration time of 1 sec. This sampling rate and resolution would resolve rapid (1–10 sec) small-amplitude (1–3 Pa) pressure disturbances like those associated with dust devils.

The mission would use a Vaisala Barocap pressure sensor like those developed and tested for the MPL Mars Volatiles and Climate Surveyor (MVACS) instrument suite and the Phoenix Scout mission. This pressure sensor would have a mass of 45 gm and dimensions of 60 × 40 × 25 mm and require <100 mW for continuous operations. A single pressure sample (including housekeeping data) would require 384 bits. If this is sampled at 3 Hz for 5-minute periods every half hour, the data volume would be 14.4 Mbit/sol.

Atmospheric Temperature

Thermocouples (TCs) to measure the atmospheric temperature would be mounted at 0.25, 0.5, and 1.0 m above the base of the mast. Another pair of sensors would be deployed on the ground. The reference junctions for the TCs would be located on an isothermal block (IB), whose temperature would be recorded by a precision platinum resistance thermometer (PRT). The TCs have been used in previous Mars landers and would be built by JPL. The IB and its PRT would be incorporated into the base of the wind sensor at the top of the ATM mast.

Each TC assembly would have a mass of <10 gm and dimension of 30 × 45 × 2 mm. The total system would require <90 mW for continuous operation. To resolve rapid temperature variations, TCs must be sampled at 0.2–1 Hz. A single temperature sample would include the five TCs, the IB PRT, and one reference (zero point) TC mounted on the IB PRT. Each measurement would be recorded as a 16-bit word. If the sampling rate is 1 Hz, the data rate would be 128 bits per second (bps). If samples are collected for 5 minutes every 30 minutes, the total data volume would be 2.64 Mbit/sol.

Hot-wire Anemometer

The horizontal wind velocity at the top of the mast would be monitored by a directional hot-wire anemometer. Its configuration and principle of operation are shown in Figure 3-5. The MVACS-derived control circuit maintains the hot wire at 100°C above ambient atmospheric temperature, and the wind speed would be determined by measuring the power needed to maintain the hot wire at this temperature. The wind sensor circuit would use ambient atmospheric temperature measurements from a pair of TCs that are mounted between the wind sensor support disks, just outside of the direction TCs. The two TC arrays would be mounted 180° apart so that one is always upstream, uncontaminated by the warm plume.

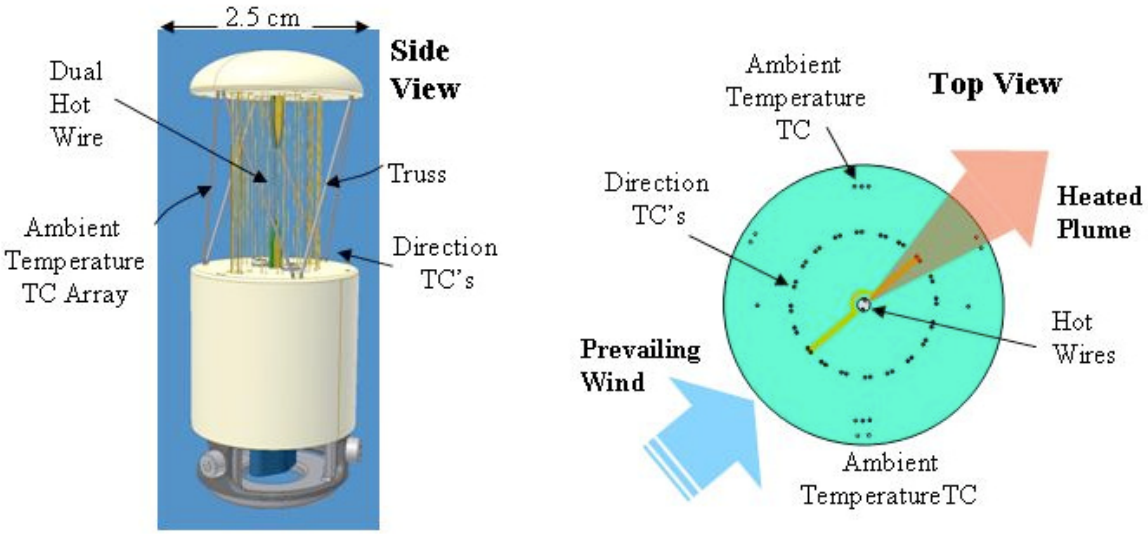

Figure 3-5. Hot-wire Anemometer Details and Operational Principle

The direction of the heated plume from the sensor's hot wires is detected by an array of 20 TCs surrounding the hot wires, which yield a directional resolution of ±9°. These TCs are identical to those used to sense the atmospheric temperature, but are connected so that they measure the temperature difference between opposite sides of the hot wire instead of the ambient temperature.

The wind velocity sensor uses a pair of hot-wire elements connected in parallel to provide redundancy. The hot wires are supported on tapered posts that are inserted through the centers of a pair of 1 mm thick fiberglass disks that form the top and bottom of the sensor, separated by a truss consisting of six 0.5 mm stainless steel wires. This disk-truss structure provides support and introduces minimal dynamical obstruction or thermal contamination.

The wind velocity sensor has a mass of 30 gm and dimensions of 25 × 25 × 75 mm, and requires 300 mW for continuous operation. Like temperatures, wind velocities must be sampled at 0.2–1 Hz to resolve convection, dust devils, and other rapidly varying phenomena. Each wind sample includes the hot-wire voltage and current, two ambient TCs, and 10 outputs from the directional TCs.

When each of these 14 values is digitized with a 16-bit ADC and sampled at 1 Hz, the raw data rate is 224 bps. If the wind direction is determined on board, the data rate would fall to 80 bps. For this case, if data is collected for 5-min periods at 1 Hz every 30 minutes, the total data volume would be 1.2 Mbit/sol.

For MPL-MVACS, extensive tests were conducted in the Mars Aeolian Facility at NASA Ames (with blowing dust) and in Mars chambers at JPL. These tests confirmed that the instrument was both robust and reliable, producing accuracies of ~10% at wind speeds between 0.1 and 100 m/s at Mars-like pressures and temperatures. The MVACS wind velocity sensor survived 600 g's in pre-flight testing.

Table 3-5. ATM (P, T, W)

Item	Value	Units
Type of instrument	Meteorology package	
Number of channels	20	
Size/dimensions (for each instrument)	0.1 x 0.1 x 0.1	m x m x m
Instrument mass **without** contingency (CBE*)	1.5	kg
Instrument mass contingency	67%	%
Instrument mass **with** contingency (CBE+Reserve)	2.5	kg
Instrument average power **without** contingency	2	W
Instrument average power contingency	50%	%
Instrument average power **with** contingency	3	W
Instrument average science data rate^ **without** contingency	9.6	kbps
Instrument average science data^ rate contingency	35%	%
Instrument average science data^ rate **with** contingency	13	kbps
Sensitivity	P=1–3 Pa, T=0.1 K, W=0.1 m/s	–
Instrument fields of view (if appropriate)	N/A	degrees
Pointing requirements (knowledge)	N/A	degrees
Pointing requirements (control)	N/A	degrees
Pointing requirements (stability)	N/A	deg/sec

*CBE = Current best estimate

^Instrument data rate defined as science data rate prior to on-board processing

Potential Additional Instruments

The following instruments are not in any of the MGN options, but could potentially be added to some MGN mission architecture options if budget were available and accommodation on the lander were possible. There is a possibility that a heat flow probe could be contributed by DLR. Contributions of instruments needed to meet the threshold science could potentially make additional budget available for other secondary science instruments. In general, mission architectures utilizing powered descent landers are expected to have greater flexibility in accommodating additional instruments than airbag lander. This is due to the airbag landers inherent tighter constraints on volume, driven by the packaging requirements of the airbags.

Geophysical Instruments

Heat Flow Probe

A heat flow probe (HP^3) would penetrate a substantial thickness (≥3 m) of the regolith of Mars while trailing a tether carrying thermal sensors to measure martian heat flow. Additional data delivered by the instrument would describe thermophysical and strength properties of the regolith to investigate local stratigraphy, and soil dielectric properties that are diagnostic of small concentrations of water or ice that might be present in the regolith.

The IDA would deploy the heat flow unit from its stowed location on the lander to the surface of Mars. A tether would provide the power and data connection between the heat flow unit and the WEM.

At the core of the HP^3 system is an electromechanical penetrometer (mole) that would travel downward into the regolith by soil displacement through the action of an internal hammering mechanism. Impacts from the mechanism would accelerate the mole forward while the recoil force is reacted by wall friction to the surrounding soil, allowing net forward motion. Depths of several meters might be reached in cumulative operating durations of a few hours, depending on soil compaction properties. The instrumented mole

consists of a leading compartment (tractor mole) housing the electromechanical hammering mechanism and a payload compartment (trailer mole) with a short flexible link connecting the two. This two-body configuration has an advantage over a “monolithic” mole in that the two units can be stored perpendicularly to one another, offering a compact stowage configuration. The two-body configuration also allows the tractor mole to deflect through a wider angle around an obstruction.

The HP^3 would be supplied by the DLR and is a version of the HP^3 developed by DLR for BepiColombo and ExoMars. The tractor mole is based on the Planetary Underground Tool (PLUTO) flown on Beagle-2. The two-body HP^3 has been under development since 2003.

The tractor mole carries a suite of sensors that would monitor the acceleration and tilt of the mole. The depth of penetration could be calculated from the integrated acceleration and deflection from vertical. However, errors accumulate quickly with depth; therefore, the payout of the tether would be monitored for a better depth measurement.

Given the known impulse of the hammer, the force and reaction of the device would allow the measurement of the resistance of the soil, resulting in a measure of the soil mechanical properties.

Thermistors are embedded in the tether and would be used to monitor the temperature gradient in the hole every hour for one full Mars year. There would be 20 thermistors providing 16 bits/hr for an average data rate of 8 kbit/sol.

The tether is made of multiple layers of kapton with a layer of thin copper conductors. It has been designed to provide a poor thermal conduction route in order to minimize the effect of the tether on the measurement. A mini-WEM attached to the HP^3 housing would contain electronics for reading the thermistor outputs.

The mole has heaters so that it could monitor the temperature rise and decay of the surrounding soil in response to a heat pulse. These measurements would be used to infer the thermal conductivity of the material with depth. Based on expected regolith properties, the hole is expected to remain open after penetration. It is essential that the air in the hole not be disturbed. For that reason, the IDA would hold the surface unit in position while the mole is operating to seal the top of the hole. The unit would have outriggers that would steady it after the IDA is removed. Details of the HP^3 are provided in Table 3-6.

Table 3-6. HP^3

Item	Value	Units
Type of instrument	Heat flow probe	
Number of channels	40	
Size/dimensions (for each instrument)	0.35 x 0.28 x 0.22	m x m x m
Instrument mass **without** contingency (CBE*)	1.5	kg
Instrument mass contingency	33%	%
Instrument mass **with** contingency (CBE+Reserve)	2	kg
Instrument average power **without** contingency	2.6	W
Instrument average power contingency	35%	%
Instrument average power **with** contingency	3.5	W
Instrument average science data rate^ **without** contingency	0.002	kbps
Instrument average science data^ rate contingency	1525%	%
Instrument average science data^ rate **with** contingency	0.036	kbps
Sensitivity	0.005	K precision
Instrument fields of view (if appropriate)	N/A	degrees
Pointing requirements (knowledge)	N/A	degrees
Pointing requirements (control)	N/A	degrees
Pointing requirements (stability)	N/A	deg/sec

*CBE = Current best estimate

^Instrument data rate defined as science data rate prior to on-board processing

Electromagnetic Sounder

The EMS would measure the subsurface electrical conductivity from 100 m to 100 km depth. The temperature structure and depth to or absence of groundwater could be inferred from the EMS measurements.

The EMS consists of two electrodes that must make electrical contact with the ground. The electrodes are on the end of two 2 m long booms that are deployed at right angles to each other or at the end of 20 m long ribbon cables that are deployed ballistically with spring-loaded bobbins. Two magnetometers per lander would be used to monitor magnetic fields.

The EMS is a passive instrument that uses ambient EM energy to probe the electrical properties of the outer layers of Mars. It has the greatest penetration of any method other than seismology. Magnetotellurics and geomagnetic depth sounding could be inverted for electrical conductivity as a function of depth. This in turn could be combined with laboratory measurements to constrain the temperature and composition of the subsurface materials.

The data rate would be 5–10 Mbit/sol, the mass is estimated to be 2.3 kg, and the power required is estimated to be 3.9 W. The required sensitivity is 10 pT/sqrt(Hz), 100μV/m/sqrt(Hz) at 1 Hz. The cost is estimated to be $8M. Further details can be found in Table 3-7.

Table 3-7. Electromagnetic Sounder

Item	Value	Units
Type of instrument	Electromagnetic sensor	
Number of channels	15	
Size/dimensions	two 0.2 x 0.2 x 0.1 (stowed) probes, one 3U electronics board	m x m x m
Instrument mass **without** contingency (CBE*)	4	kg
Instrument mass contingency	38%	%
Instrument mass **with** contingency (CBE+Reserve)	5.5	kg
Instrument average power **without** contingency	3.9	W
Instrument average power contingency	41%	%
Instrument average power **with** contingency	5.5	W
Instrument average science data rate^ **without** contingency	0.057	kbps
Instrument average science data^ rate contingency	100%	%
Instrument average science data^ rate **with** contingency	0.115	kbps
Sensitivity	1 pT/sqrt(Hz), 100 uV/m/sqrt(Hz) @ Hz	
Instrument fields of view (if appropriate)	N/A	degrees
Pointing requirements (knowledge)	N/A	degrees
Pointing requirements (control)	N/A	degrees
Pointing requirements (stability)	N/A	deg/sec

*CBE = Current best estimate

^Instrument data rate defined as science data rate prior to on-board processing

Atmospheric Instruments

Sonic Anemometer

A sonic anemometer would measure the 3D wind velocity at the top of the mast. Its configuration is shown in the Figure 3-6. The instrument would consist of six sound transducers arranged in pairs along three mutually orthogonal axes. The flight time of sound between opposing pairs of sensors (+ and – velocity along 3 axes = 6 directions) would be measured and used to solve for the 3D wind velocity vector.

Coupling between the sonic sensor/actuator and the atmosphere at Mars requires a different transducer compared to Earth due to the low atmospheric pressure (Mars <= 0.6 % Earth). An electrostatic transducer is available and has been tested to operate under Mars-like conditions of pressure, temperature, and dust.

The advantages of the sonic anemometer over the hot-wire anemometer flown on previous missions is the ability to measure the 3D wind vector compared to the horizontal 2D wind vector and the ability to operate at 8 Hz or higher while the response time of the TCs and heater wire limits the hot-wire anemometer to around 1 Hz.

The mass of the instrument would be 1.0 kg with an average power of 3.0 W. The data rate would be 9.6 kbits/sec in the worst case.

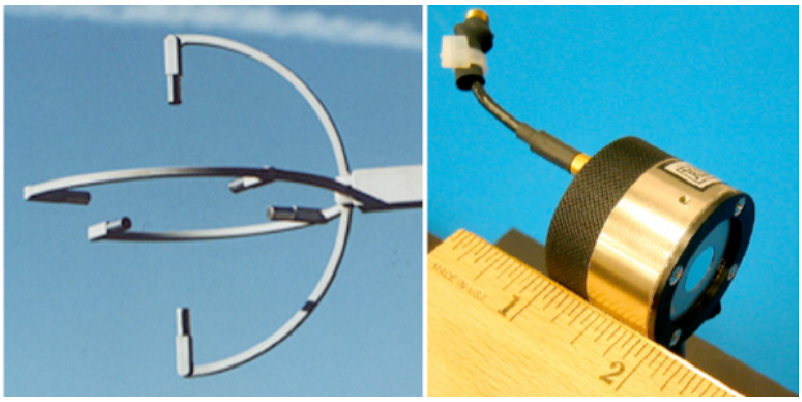

Figure 3-6. Sonic anemometer (left) and a photograph of the electro-static transducers that enable sonic anemometry at Mars (right).

Atmospheric Humidity

In-situ measurements of the near-surface humidity would be made with a Vaisala Humicap sensor contributed by the Finnish Meteorological Institute (FMI). It would be mounted 0.5 m above the base of the mast. Humicaps sensors would determine the humidity as water vapor is adsorbed in a polymer sandwiched between capacitive electrodes. They typically have accuracies of ±3% relative humidity at temperatures between 190–350 K. They work at lower temperatures, but their response time increases from 5 minutes to >30 minutes as temperature decreases from 200 K to 170 K. The MSL REMS "Digihum" implementation, which includes the Humicap sensor and the electronics for digitizing the Humicap data has been baselined. Because the Digihum sensor head would be exposed to the Mars environment, it has been qualified from 150–290 K. The output of these sensors would be identical to that of the Barocap pressure sensors described above. It consists of a frequency signal between 3 and 20 kHz that is monitored by a 10 MHz counter. This frequency data would be read by the electronics board in the WEM.

The humidity sensor has a mass of 16 gm and dimensions of 16 × 16 × 35 mm, and requires <100 mW for continuous operation. A single humidity sample (including housekeeping data) requires 384 bits. If the humidity is measured twice an hour throughout the sol, the total data volume would be 19.2 kbit/sol.

Dust Opacity

As on Viking, MPF, and MER, the total column dust optical depth could be monitored by direct observation of the Sun through special solar filters on the IDC. In order to do this, the IDC would be outfitted with a set of filters, using the same design as was done on Pancam.

Dust Concentration

The local concentration of airborne dust would be measured by a pair of dust impact sensors. The atmospheric dust sensor (ADS) is a simplified version of the impact stage of the GIADA dust sensor, currently flying on Rosetta; another version flew on Beagle-2. It measures the momentum and rate of impact of airborne dust and sand with a piezoelectric sensing film, which generates a charge when grains impact onto it. This charge is amplified and captured by integral electronics. The sensor then produces an analog voltage output proportional to the grain momentum. This voltage is maintained until the sensor is reset via a logic line.

Two cylindrical dust sensors would be mounted on the mast, one near the bottom and the other near the top. Since the sensor measures particle momentum, simultaneous measurements of wind speed are useful in interpreting the sensor data in terms of particle mass and velocity. Each of the sensors has a mass of 15 gm, with a diameter of 20 mm and a height of 40 mm. The two sensors require <120 mW for continuous operation. The dust sensor is monitored at 4 kHz, and counts are accumulated for sampling periods ranging from 1–5 minutes. This would yield a data rate of 23 kbits/sol. Further details of the dust sensor instrument are provided in Table 3-8.

Table 3-8. Atmospheric Dust Sensors (Two)

Item	Value	Units
Type of instrument	Dust sensor	
Number of channels	4	
Size/dimensions (for each instrument)	0.04 height x 0.02 diameter	m x m
Instrument mass **without** contingency (CBE*)	0.015	kg
Instrument mass contingency	33%	%
Instrument mass **with** contingency (CBE+Reserve)	0.02	kg
Instrument average power **without** contingency	0.12	W
Instrument average power contingency	33%	%
Instrument average power **with** contingency	0.16	W
Instrument average science data rate^ **without** contingency	0.0003	kbps
Instrument average science data^ rate contingency	30%	%
Instrument average science data^ rate **with** contingency	0.0003	kbps
Sensitivity	N/A	
Instrument fields of view (if appropriate)	N/A	degrees
Pointing requirements (knowledge)	N/A	degrees
Pointing requirements (control)	N/A	degrees
Pointing requirements (stability)	N/A	deg/sec

*CBE = Current best estimate

^Instrument data rate defined as science data rate prior to on-board processing

Flight System

The flight system for the proposed MGN mission would include three unique flight elements for all options considered, except for the MOOs, which only have two unique flight elements. The flight elements would be a lander, an entry system, and a cruise stage. The MOO options would include just the entry system and lander, and assume that the primary flight element would provide the functionality typically provided by the cruise stage.

Both the powered descent and airbag landers would be designed to survive at least one martian year on the surface. Each lander would house a command and data handling (C&DH) subsystem, which would not only operate during the primary science phase while on the surface, but also during the cruise and entry phases of the mission. This architecture, similar to what was used by the MPF, MER, and Phoenix missions, could reduce overall cost, mass, and power needs by focusing the complexity associated with the majority of the electronic systems of the entire flight system into a single flight element.

Science requirements on landing-site selection are assumed to be minimal (~3,000 km lander separation and near the Tharsis region). Since exact landing location is not a driver from a science standpoint, no guided entry or pinpoint landing would be required, and 100 km by 20 km landing ellipses would be acceptable. Safe landing ellipses could be examined and certified using Mars Reconnaissance Orbiter (MRO) High Resolution Imaging Science Experiment (HiRISE) images. This flexibility (from a science perspective) would allow landing site elevation and latitude to drive landing site selection for both the powered descent and airbag architectures.

Note that for the mission architectures that contain more than one station (lander), it is assumed that the flight systems are exact copies of each other. Therefore, the number of landers would not impact the flight system design with the exception of the launch configuration, deployment of the free flyers, and the common carrier element.

The two- and three-lander, free flyer architectures (for both airbag and powered descent landers) would require the landers to be mounted on a dispenser. The dispenser would allow the landers to be launched on a single launch vehicle, and be released from the upper stage (to which the dispenser would be attached) with appropriate separation from each other. This dispenser would also properly mount the landers to handle launch loads. Figures 3-7 and 3-8 show notional illustrations of the dispenser for two- and three-lander architectures. The three-lander dispenser configuration could also apply to the three-lander common carrier architecture.

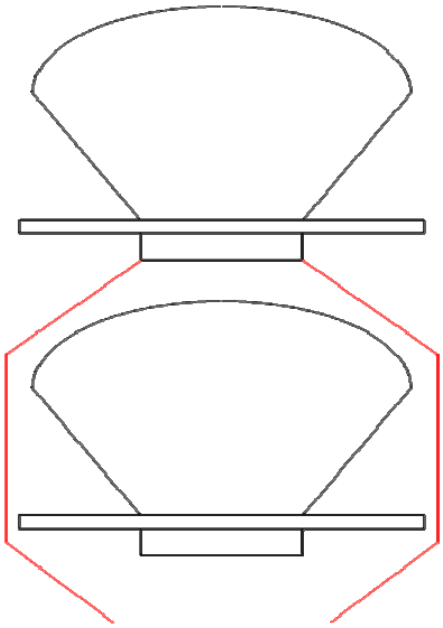

Figure 3-7. Concept of a Two-Lander Stacked Configuration

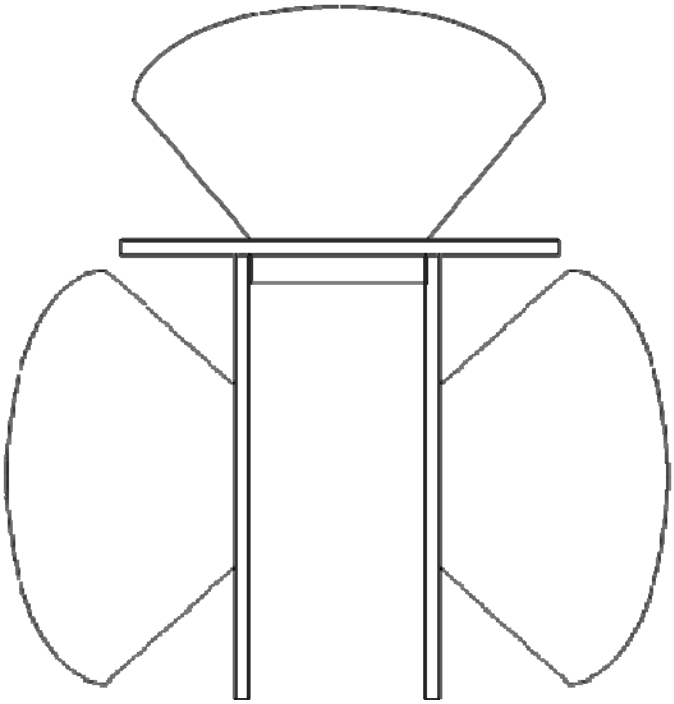

Figure 3-8. Concept of a Three-Lander Dispenser or Common Carrier Configuration

Airbag Landers

The airbag lander architectures would have a terminal descent that would utilize solid RAD rockets with a MER airbag system and a tetrahedron lander. This EDL approach would be supported by a 100% success rate (MPF, and the two MERs). The C&DH subsystem would be housed completely on the lander, which would focus the electronics complexity on a single flight element.

Lander Subsystems

The ACS hardware on the lander would include the IMU. The primary structure of the lander would be based on MPF and MER heritage, with three deployable petals. Other deployments include the IDA and ATM mast (the solar arrays are mounted on the pedals and therefore deployed with them). The ability to minimize nighttime science data collection (SEIS only) and the warm electronics module (WEM) would allow the lander to survive worst-case martian winter nights.

Cruise Approach

Three cruise architectures were considered for the airbag lander architecture: free flyers, secondary payload, and common carrier. The free flyer architecture would require the flight system to include a separate cruise stage flight element. This approach would be very similar to the MER cruise stage design. The cruise stage would consist of an aluminum ring-like primary structure with solar panels mounted on the outer ring. A star scanner and sun sensors would determine the attitude of the vehicle. A hydrazine propulsion system would be used for maneuvering the flight system from Earth to Mars. X-band, low-gain and medium-gain antennas would be used for telecommunications. While the main flight computer would be on the lander, the cruise stage would have power electronics. After being placed in Earth orbit, the cruise stage would deliver (spin stabilized) the flight system to Mars and release the entry system to begin the EDL sequence.

The flight system could potentially be carried as a secondary payload on a MOO. No cruise stage flight element would be required if this cruise architecture were pursued. This approach would be advantageous because the overall cost would be reduced by sharing the launch vehicle with another

mission and removing the cruise stage from the flight system. The launch vehicle for the MOO would likely need to be more capable than the primary mission would nominally require. For example, the launch vehicle would change from an Atlas V 521 to an Atlas V 531 or 541.

A cruise stage would also not be required if the three-station mission utilized a common carrier to deliver the flight systems to Mars. The three landers would be launched in a stacked configuration and remain within the common carrier until entry minus 15, entry minus 8, and entry minus 1 days. The common carrier would be similar to a large cruise stage. It would support the three flight systems structurally, supply power from its solar arrays, and contain a propulsion system, thermal radiators, and basic attitude determination and telecommunication components. The common carrier would release the landers with a spin-ejection mechanism.

Entry System

The proposed MGN entry system design for airbag landers is based on the MPF and MER designs. This design could be made independent of the cruise architecture. The entry vehicle would separate from the cruise stage and maintain attitude alignment through spin stabilization. MGN would enter the martian atmosphere ballistically with no active control. The mechanical design of the vehicle consists of an aeroshell that would protect the lander during cruise and hypersonic entry phase, and a supersonic parachute to slow the entry vehicle to a required velocity/altitude prior to the firing of the RAD rockets and eventual free fall of the MGN airbag lander. The aeroshell mechanical design is composed of a heatshield and backshell, which are protected by a thermal protection system (TPS) such as SLA-561. The mission would use the same aeroshell diameter (2.65 m) as was used on the MPF, MER, and Phoenix flight projects. Also similar to MPF, MER, and Phoenix, the supersonic parachute would be disk-gap-band, which would preserve the Viking chute design. The IMU and descent sensor (for altitude) would be used to trigger the parachute opening and later the airbag deployment. An IMU would be on both the aeroshell and the lander and the descent sensor would be on the aeroshell. The only other hardware present on the entry system would be a UHF antenna for EDL communications to an orbiting asset. Power, C&DH, ACS, and telecommunication functions during entry would be performed by lander subsystems.

Powered Descent Landers

The powered descent lander architectures would have a hydrazine monopropellant propulsion system for terminal descent. These options would benefit from this architectural approach by using a single propulsion subsystem for cruise and EDL. By scarfing the trajectory correction maneuver (TCM) and reaction control system (RCS) thrusters through the backshell, the need for a second propulsion system on the cruise stage would be eliminated, saving significant mass and cost. Similarly, one of the two small deep space transponders (SDSTs) that would typically be required on each cruise stage (for redundancy) would instead be on the lander, where it could provide the hardware needed to conduct the radio science experiment and provide emergency X-band direct-to-Earth (DTE) communications. Like the airbag lander, the powered lander would be a “smart lander” that houses the C&DH subsystem.

Lander Subsystems

The ACS hardware on the lander would include the IMU (which would be used during cruise and EDL) and the landing radar, which would be operational during the descent phase. The lander propulsion system would be a regulated monopropulsion hydrazine system using gaseous helium as a pressurant. The primary structure of the lander would be made of aluminum and comprised of a lander deck supported by landing legs and struts. The lander would require three deployable legs. Other deployments would include the solar arrays, IDA, and ATM mast. A power system with ultraflex solar arrays should enable landing site latitudes up to 20 North. The ability to minimize nighttime science data collection (SEIS only), and a tight thermal enclosure for the avionics (which would minimize needed heater power) should allow the lander to survive worst-case martian winter nights.

Cruise Approach

Two cruise approaches were considered for the powered landers: secondary payload and free flyers. Targeting a MOO, the lander would piggy-back as a secondary payload on another mission. This approach could only accommodate one lander and would not require a cruise. The lander and entry

system designs would not be fundamentally impacted by this approach, assuming that the host primary flight element would provide the functionality of a cruise stage.

The free flyer approach would require each flight system to contain a cruise stage that would deliver the lander to Mars. The cruise stage structure would essentially be a launch adapter ring with necessary cruise hardware attached. The solar array deployment mechanisms would be the only significant mechanisms on the cruise stage. The solar arrays would support operation of the spacecraft until approximately five minutes prior to entry. The cruise stage would have no power electronics on board. The cruise stage telecommunications subsystem would be solely X-band and contain a low-gain patch antenna, fixed medium-gain antenna, and SDST as the primary components. The attitude control subsystem on the cruise stage would perform attitude determination by the use of sun sensors, star trackers, and the landers IMU. The cruise stage would be 3-axis stabilized. The cruise stages would not have C&DH or propulsion subsystems, rather the landers' C&DH and propulsion subsystems would be used during cruise and EDL. The TCM and RCS thrusters would be scarfed through the entry system's backshell to allow the lander's propulsion system to also be used during the cruise phase.

Entry System

The MGN entry system design for powered landers is based on the Phoenix design. The entry vehicle would separate from the cruise stage and rely on the RCS thrusters for the attitude alignment approximately five minutes prior to entry point. This entry system could potentially utilize the active control capability during entry; however, similar to the Phoenix architecture, MGN would enter the martian atmosphere ballistically with no active control. The mechanical design of the vehicle consists of an aeroshell that would protect the lander during cruise and hypersonic entry phase, and a supersonic parachute to slow the entry vehicle to a required velocity/altitude prior to powered terminal descent. The aeroshell mechanical design is composed of a heatshield and backshell, which are protected by TPS such as SLA-561. The mission would use the same aeroshell diameter (2.65 m) as was used on the MPF, MER, and Phoenix flight projects. Also, similar to MPF, MER, and Phoenix, the supersonic parachute would be disk-gap-band, which would preserve the Viking chute design. The IMU and landing radar would both also be carried by the lander.

The only other hardware present on the entry system would be a UHF antenna for EDL communications to an orbiting asset. Power, propulsion, C&DH, ACS, and telecommunication functions during entry would be performed by lander subsystems.

Concept of Operations and Mission Design

The MGN architectures would have very similar concepts of operations and mission designs. The primary differentiators would include the number of stations and the timing of lander separation. The free flyer cruise architecture would have separation occur just after launch. The cruise and EDL operations for this architecture would therefore be replicated for each spacecraft. The common carrier cruise architecture would have separation occur just prior to EDL. For the common carrier approach, cruise operations would only support one vehicle, and each lander's EDL sequence would occur within hours of each other. The secondary payload cruise architecture would have separation occur just prior to EDL also. Since the lander would be carried by another primary element, the cruise operations would be handled by the primary mission.

The launch configuration for the architectures would vary based on the number of landers being launched, however, in all cases only one launch vehicle would be required. The launch would take place at the Cape Canaveral Air Force Station within an allocated 21-day launch period. The mission design for this particular Mars arrival opportunity was driven by the relatively short cruise phase and minimum entry speed for Mars EDL conditions.

The launch vehicle (ranging from a Falcon 9 to an Atlas 531, depending on landing type and number of landers) would place the flight system into a low Earth orbit. The ground stations would provide sufficient tracking while the launch vehicle continues its coast phase to a location where the interplanetary orbit injection is planned to occur. At the targeted injected state (~launch +55 min), the upper stage would

perform a trajectory injection maneuver (second burn), which would send the first spacecraft, common carrier, or the primary spacecraft (with secondary payload) toward Mars.

In the free flyer architectures, each individual flight system (cruise stage, entry system, and lander) would separate from the dispenser, while the other spacecraft would remain attached to the Centaur with the adapter. Expert opinion indicated that a seven-day separation between the EDL sequences would be appropriate. Hence, to provide the proper separation between the spacecraft arrivals, the Centaur would utilize a third burn to perform a small maneuver (ΔV ~90 m/s), which would delay the Mars arrival epoch for the second spacecraft by seven days. The second spacecraft would separate from the dispenser following this maneuver. For free flyer architectures involving a third lander, the spacecraft propulsion systems would perform their own delta-V separation maneuvers (in separate directions) to distance itself from the other lander. Once all the spacecraft are separated and sent on their way to Mars, the launch vehicle would bias away from Mars in agreement with planetary protection protocols. Between 10 and 20 days following launch, all spacecraft would finish system checkout and execute the first TCM (TCM-1). This maneuver would have two purposes: to remove the launch bias and to clean up the launch dispersions. The ΔV budget of each spacecraft would allow performance of five to six more TCMs prior to Mars entry, if needed.

The common carrier architecture would launch, be released, and travel to Mars as a single element. The landers would be released at entry minus 15, entry minus 8, and entry minus 1 days out, but all arrive within hours of each other.

All architectures would follow a direct, Type I transfer to Mars with a total flight time of approximately seven months.

The data tracking and communications between Earth and the spacecraft during the cruise phase would be supported by the traditional set of Deep Space Network (DSN) stations located in Canberra, Goldstone, and Madrid. Tracking would include Doppler, ranging, and ΔDOR measurements. The data tracking for navigation would require two passes per week for each spacecraft during the cruise phase with increased tracking frequency at Mars entry minus 30 days for each of the EDLs. The tracking would normally rely on the 34 m antennas with some occasional use of 70 m antennas for EDL critical event coverage.

The 2022 landing opportunity would be favorable from an EDL standpoint. The entry velocity would not be excessively high and would avoid any global dust storm seasons. Table 3-9 shows some of the details of a representative launch window. The EDL operations for the different architectures would primarily vary based on the number of landers and cruise architecture. The landing architecture is not a significant factor since EDL would occur too quickly for the team to respond. EDL operations would be replicated for each spacecraft. The EDL separation between landers would be seven days for the free flyer architectures. The common carrier architecture, however, would have less than 12 hour EDL separation. Preliminary landing locations have been suggested for the proposed MGN mission. Several potential landing targets have been identified that would be compatible with the predicted landing ellipse of 100 km $\times$ 20 km, as well as rock abundance, elevation, and surface slope requirements similar to those derived for the Phoenix mission.

Initial surface operations for all architectures considered would include deployments of the lander solar array, robotic arm, and atmospheric instrument suite (ATM) mast, followed by placement of the seismometer on the surface. Once the seismometer is deployed, the robotic arm would not need to be used again for the remainder of the mission, and there would be no further tactical operations. Each lander would then operate continuously as a simple monitoring station with routine operations.

Science data would be relayed twice daily from each lander via an ultra-high frequency (UHF) telecommunications link to an existing orbiting asset. Downlink to Earth would be based on the asset's DSN schedule. In addition to the relay communications link, there would be a weekly one-hour radio science X-band two-way Doppler/ranging link between the DSN and lander (one lander each week). This link would support a carrier-only signal and could not be used for commanding or data return. The ground data system would be relatively simple and the science team would be small for the baseline (science floor payload).

Table 3-9. Earth-Mars 2022 Type I Trajectory with Launch Window

Day	LD	AD	TOF (day)	C3 (km2/sec2)	DLA (deg)	RLA (deg)	VHP (km/sec)	DAP (deg)	RAP (deg)	VENTRY (km/sec)	Ls (deg)	SEP (deg)
1	220907	230408	213	18.641	49.333	57.02	3.41	-23.351	46.246	5.99617	47.914	78.849
2	220908	230408	212	18.57	48.419	56.358	3.404	-22.795	46.686	5.99276	47.914	78.849
3	220909	230408	211	18.54	47.523	55.697	3.399	-22.259	47.094	5.98993	47.914	78.849
4	220910	230408	210	18.549	46.646	55.039	3.395	-21.742	47.472	5.98766	47.914	78.849
5	220911	230408	209	18.595	45.786	54.387	3.392	-21.243	47.822	5.98596	47.914	78.849
6	220912	230408	208	18.679	44.942	53.744	3.389	-20.759	48.144	5.98426	47.914	78.849
7	220913	230408	207	18.799	44.115	53.112	3.387	-20.29	48.44	5.98312	47.914	78.849
8	220914	230408	206	18.956	43.304	52.492	3.386	-19.833	48.712	5.98256	47.914	78.849
9	220915	230408	205	19.149	42.508	51.886	3.385	-19.389	48.959	5.98199	47.914	78.849
10	220916	230408	204	19.378	41.73	51.297	3.384	-18.955	49.183	5.98143	47.914	78.849
11	220917	230408	203	19.643	40.967	50.725	3.384	-18.531	49.384	5.98143	47.914	78.849
12	220918	230408	202	19.945	40.221	50.172	3.385	-18.116	49.563	5.98199	47.914	78.849
13	220919	230408	201	20.283	39.492	49.639	3.385	-17.708	49.721	5.98199	47.914	78.849
14	220920	230408	200	20.659	38.78	49.127	3.386	-17.308	49.858	5.98256	47.914	78.849
15	220921	230408	199	21.072	38.086	48.637	3.388	-16.914	49.975	5.98369	47.914	78.849
16	220922	230408	198	21.523	37.409	48.169	3.389	-16.525	50.073	5.98426	47.914	78.849
17	220923	230408	197	22.013	36.75	47.725	3.391	-16.14	50.15	5.98539	47.914	78.849
18	220924	230408	196	22.542	36.11	47.304	3.393	-15.76	50.209	5.98652	47.914	78.849
19	220925	230408	195	23.112	35.489	46.907	3.395	-15.383	50.248	5.98766	47.914	78.849
20	220926	230408	194	23.722	34.886	46.534	3.398	-15.009	50.27	5.98936	47.914	78.849
				23.722						**5.99617**		

Planetary Protection

In accordance with NPR 8020.12C, the proposed MGN mission is expected to be a Planetary Protection Category IVa mission. Accordingly, the MGN project would demonstrate that its mission meets the Category IVa planetary protection requirements per NPR 8020.12C, Appendix A.2 and the landers would not go to special regions. The official planetary protection category of the mission would be formally established by the NASA Planetary Protection Officer (PPO) in response to a written request from the MGN Project Manager, submitted by the end of Phase A.

The proposed MGN mission plans to assemble the spacecraft hardware in Class 8 cleanroom facilities with appropriate controls. The bioburden requirements would be met by using a combination of cleaning and dry heat microbial reduction (DHMR). Cleaning would be done by either alcohol wipe or precision cleaning compatible hardware. DHMR would be used for portions of the spacecraft having large surface areas (e.g., multilayer insulation [MLI], parachute), surfaces that are difficult to clean (e.g., honeycomb structures, batting insulation), and portions of the spacecraft having large accountable encapsulated non-metallic volumes (e.g., thermal protection system of the aeroshell). Credit would be taken for high-temperature cures and manufacturing processes whenever possible. The MGN mission would perform bioassay sampling of the spacecraft hardware at last access to determine the level of bioburden present on the spacecraft at launch and to determine the diversity of the microbial population. There would also be bioassays performed at intermediate steps to monitor the spacecraft during assembly and test activities. MGN personnel would perform the sampling as directed by the NASA PPO office for the PPO's independent verification bioassays. An entry heating analysis would be performed, similar to the analysis performed for past Mars missions (up to and including Mars Science Laboratory), to determine which outboard surfaces of the aeroshell's heatshield and backshell would be sterilized by heating to greater than 500°C during Mars entry. If entry heating is found to be insufficient to sterilize the entire outboard surface of the aeroshell, then additional measures would be taken to protect the aeroshell and lander from recontamination by the cruise stage and launch vehicle during launch decompression. An entry heating and breakup analysis, similar to the analysis performed by the Phoenix project, would be performed to demonstrate that the cruise stage would be sterilized by heating to greater than 500°C during Mars entry. If MGN is unable to demonstrate adequate heating, then the cruise stage would undergo cleaning and DHMR processes as needed to meet the bioburden requirements. The entry heating and breakup analysis would be reported in the pre-launch planetary protection report. The organic materials list would be compiled and the required samples collected for archiving. The organic materials list would also be reported in the pre-launch planetary protection report. The organic materials samples would be archived at JPL by the Biotechnology and Planetary Protection Group. The non-impact requirements would be demonstrated by analyses performed by the navigation team at JPL, similar to the analyses performed in the past by the MPF, MPL, and MER projects. The navigation team at JPL would also identify the location of the landing point on Mars. That location would be reported in the planetary protection end-of-mission report.

Risk List

A detailed consideration of mission risks was not undertaken as part of this study, other than what is discussed elsewhere in the report.

4. Development Schedule and Schedule Constraints

Development Schedule and Constraints

No particular schedule constraints exist for this mission other than those that would normally apply to all Mars missions. The mission schedule for this study assumes that a relay orbiter would be available to support the proposed MGN mission. Two representative timelines for a Mars mission of this type would be characterized by Phase durations shown in Table 4-1. The schedule for options A through E represents a potential New Frontiers class mission. The schedule for options F through I represents a potential Discovery class or Mission of Opportunity mission. These two representative schedules were used for the various architectures as a simplifying assumption in this study.

Table 4-1. Representative Mission Schedule Phase Durations

Project Phase	Options A-E Duration (Months)	Options F- I Duration (Months)
Phase A – Conceptual design	9	9
Phase B – Preliminary design	10	10
Phase C – Detailed design	22	18
Phase D – Integration & test	20	18
Phase E – Primary mission operations	30	30
Phase F – Extended mission operations	4	4
Total development time Phase B–D	52	46

As with any Mars mission, a favorable 21-day launch opportunity for Type I/II trajectories occurs approximately every two years.

Technology Development Plan

No technology development would be required for the baseline mission. Therefore, no technology development plan is provided here.

5. Mission Life-Cycle Cost

Costing Methodology and Basis of Estimate

JPL's Advanced Project Design Team (Team X) generates a most likely cost for the JPL standard work breakdown structure (WBS) that may be tailored to meet the specific needs of the mission being evaluated. These estimates are done at WBS levels 2 and 3 and are based on various cost estimating techniques. These methods are not exclusive to each other and are often combined. The various estimating techniques consist of grassroots techniques, parametric models, and analogies. The models for each station at Team X have been built (total of about 33) and validated, and they are each owned by the responsible line organization. The models are under configuration management control and are utilized in an integrated and concurrent environment, so the design and cost parameters are linked. These models are customized and calibrated using actual experience from completed JPL planetary missions. In applying these models, it has been found that the resultant total estimated Team X mission costs have been consistent with mission actual costs.

The cost estimation process begins with the customer providing the base information for the cost estimating models and defining the mission characteristics, such as:

- Mission architecture
- Payload description
- Master equipment list (MEL) with heritage assumptions
- Functional block diagrams
- Spacecraft/payload resources (mass [kg], power [W])
- Phase A–F schedule
- Programmatic requirements
- Model specific inputs

Most of the above inputs are provided by the customer through a Technical Data Package. For Decadal Survey missions, the following specific guidelines were also followed:

- Reserves were set at 50% for Phases A–D.
- Reserves were set at 25% for Phase E.
- The launch vehicle cost was specified in the ground rules.

Cost Estimates

Team X did not generate costs for any of the MGN mission options as part of this trade study effort. Rather, the cost estimates provided in this section are based on previous Team X cost estimates for proposed MGN missions. These existing cost estimates were then modified to reflect the various architectures of this trade study. The existing Team X studies included powered-descent landers, airbag landers, as well as common carrier and free flyer architectures. The studies covered single-lander architectures as well as three-lander architectures. Due to the fact that all Team X cost estimates include recurring and non-recurring costs, it was also possible to generate cost estimates for MGN architectures with two stations.

All Team X cost estimates were inflated to FY2015 using the NASA New Start Inflation Index. Phase A–D reserves for each architecture were set to 50%, and Phase E–F reserves were set to 25%, per the Planetary Science Decadal Survey ground rules

The previous Team X studies that were used in generating MGN cost estimates were originally conducted between 1–3 years earlier. For this reason, it was necessary to update some of the cost estimates by running updated cost models. This was done for the following elements of the WBS:

- Project management (WBS element 1.0)
- Project systems engineering (WBS element 2.0)
- Mission assurance (WBS element 3.0)

Science (WBS element 4.0) costs during development were assumed to be constant across all architectures studied, at $10M (FY 2015). This was driven by the fact that all options also were assumed to have the same payload. However, science costs during operations scaled with the number of stations.

Education and public outreach (WBS element 11.0) costs were estimated as 1% of the total project cost, less reserves, with 25% allocated during development, and 75% allocated for Phases E–F.

Launch vehicle (WBS element 8.0) costs were taken directly from the Planetary Science Decadal Survey ground rules, while launch vehicle capability was determined using the elvperf.ksc.nasa.gov website. Architectures utilizing the Atlas V 521 assumed a launch vehicle cost equal to the average of the Atlas V 511 and Atlas V 531, due to the fact that the cost of the Atlas V 521 is not specified in the Planetary Science Decadal Survey ground rules.

Flight System (WBS Element 6.0) Costs

The Team X cost data that was the basis for each multi-station architecture showed that overall, the flight system recurring costs (as a percentage of the first unit cost) ranged from approximately 35–45%.

The Dispenser cost estimate of $12M was based on quasi-grassroots estimate conducted as part of an earlier Team X study. It should be noted that there is higher cost risk associated with this estimate than other costs, due to lack of design heritage.

Costs for Ames Research Center and Langley Research Center aerothermal and aerostability analyses and arcjet testing were independently estimated at $5M (FY 2015) total.

Costs estimates for all lander C&DH subsystems were based on single-string architectures. Telecommunication subsystem cost estimates assumed redundant UHF Electra-lite and single-string X-band (DTE) systems.

Payload (WBS element 5.0) costs were estimated using previous Team X study data. Table 5-1 shows instrument costs, which represent the science floor payload (as described in the Section 1) for all architectures.

Mission operations system (MOS) (WBS element 7.0), ground data system (GDS) (WBS Element 9.0), and mission design (WBS element 12.0) costs were estimated using existing Team X study cost estimates. Development costs were relatively insensitive to the number of stations. Operations costs were driven by cruise tracking and DSN time, and again, scaled between the previous Team X studies for one and three station missions. Cost estimates for MOO mission architectures do not include DSN costs during cruise, due to the assumption that these costs would be borne by the primary mission. All MOS/GDS cost estimates assume a surface duration of one martain year.

Table 5-1. Instrument Cost Estimates ($FY15)

Instrument	Non- Recurring Cost	Recurring Cost	First Unit Cost
Seismometer	$8.1M	$5.8M	$13.9M
ATM (press., temp., wind, humidity)	$4.6M	$3.4M	$8M
Robotic arm	$5.5M	$2.5M	$8M
HazCams/NavCam	$0.4M	$0.6M	$1M
Total	**$18.6M**	**$12.3M**	**$30.9M**

Cost Caps

For the purposes of cost binning, the cost cap for a Discovery class mission in FY2015 was assumed to be ~$670M. The New Frontiers cost cap was assumed to be ~$1,010M. These values are based on principal investigator (PI)-managed cost cap and launch vehicle data from recent New Frontiers and Discovery Program announcement of opportunities (AOs), as shown in Table 5-2. The NASA New Start Inflation index and launch vehicle costs were taken directly from the Planetary Science Decadal Survey ground rules.

Based on the total project costs calculated using the methodology documented above and the cost caps assumed, only two architectures are near the expected cost caps. The single powered lander mission (Option G) is within 10% of the expected cap for a Discovery mission, and the two free flying powered landers mission (Option E) is estimated to be right at the cap for a New Frontiers mission. Table 5-3 shows total project cost estimates for all nine options.

It is important to note that the above cost estimates do not assume any foreign contributions. If likely foreign contributions for the seismometer were taken into account, the above estimates would be reduced by $20M–$50M, depending on the number of stations. Also, each of these cost estimates assume the required 50% reserves during development. For mission architectures that rely so heavily on existing technology and with heritage to flight projects (Pathfinder, MER, and Phoenix), 50% development reserves are probably excessive. If a more conventional reserve posture of 30% were assumed, the total project costs assumed above would drop by $70–140M. This reserve posture would drop the cost estimate for a three-powered descent lander network down to within 10% of the expected New Frontiers cap, not including any reductions for foreign contributions.

Table 5-2. Cost Cap Assumptions

	Discovery		**New Frontiers**	
	$FY2010	**$FY2015**	**$FY2009**	**$FY2015**
Current limit	$425M	$488M	$650M	$758M
LV cost (per PSDS ground rules)	Assumes Atlas V 401		Assumes Atlas V 551	
	$155M	$178M	$220M	$257M
Total Mission Cost	**$580M**	**$666M**	**$870M**	**$1,014M**

Table 5-3. Total Project Cost Estimates

Option	B	A	D	C	E	H	G	I	F
Total Project Cost	**1347**	**1469**	**1216**	**1195**	**1015**	**911**	**720**	**622**	**527**
Dev. Cost (Phase A-D)	**1045**	**1118**	**922**	**916**	**749**	**677**	**542**	**579**	**484**
1.0 Project Management	16	16	16	16	16	11	11	11	11
2.0 Project Sys. Eng.	29	29	29	25	25	19	19	19	19
3.0 Mission Assurance	33	35	29	29	24	21	17	18	15
4.0 Science	10	10	10	10	10	10	10	10	10
5.0 Payload System	61	61	61	48	48	36	36	36	36
6.0 Flight System	437	472	352	382	279	275	192	227	169
7.0 Mission Ops	22	22	22	21	21	20	20	13	13
9.0 GDS	21	21	21	20	20	19	19	15	15
10.0 ATLO	57	63	59	46	44	30	28	27	25
11.0 EP&O	3	3	2	2	2	2	1	1	1
12.0 Mission and Nav Design	8	13	13	11	11	8	8	8	8
Dev. Reserves	348	373	307	305	250	226	181	193	161
Ops Cost (Phase E-F)	**71**	**94**	**90**	**75**	**75**	**56**	**56**	**43**	**43**
1.0 Project Management	4	4	4	4	4	2	2	2	2
2.0 Project Sys. Eng.	2	2	2	1	1	1	1	1	1
3.0 Mission Assurance	0.5	0.7	0.6	0.5	0.5	0.4	0.4	0.3	0.3
4.0 Science	22	23	23	17	17	13	13	13	13
7.0 Mission Ops	24	41	38	33	33	24	24	14	14
9.0 GDS	4	4	4	4	4	4	4	4	4
11.0 EP&O	0.5	0.7	0.7	0.6	0.6	0.4	0.4	0.3	0.3
12.0 Mission and Nav Design	0	0	0	0	0	0	0	0	0
Ops Reserves	14	19	18	15	15	11	11	9	9
8.0 Launch Vehicle	**231**	**257**	**204**	**204**	**190**	**178**	**122**	**0**	**0**
Landing Architecture	Airbag	Airbag	Powered	Airbag	Powered	Airbag	Powered	Airbag	Powered
# Stations	3	3	3	2	2	1	1	1	1
Cruise Architecture	CC	FF	FF	FF	FF	FF	FF	MOO	MOO

Option	B	A	D	C	E	H	G	I	F
Total Project Cost	**1347**	**1469**	**1216**	**1195**	**1015**	**911**	**720**	**622**	**527**
Launch Vehicle	Atlas V 521	Atlas V 531	Atlas V 511	Atlas V 511	Atlas V 501	Atlas V 401	Falcon 9	N/A	N/A
Target Class	New Frontiers	New Frontiers	New Frontiers	New Frontiers	New Frontiers	Discovery	Discovery	MOO	MOO

Key:

Red = >15% over assumed cost cap

Orange = <15% over assumed cost cap

Green = Under assumed cost cap

Blue = No cost cap assumed

Notes:

CC = common carrier

FF = free flyer

MOO = mission of opportunity

Appendix A. Acronyms

ACS	attitude control system
ADC	analog-to-digital converter
ADS	atmospheric dust sensor
AO	announcement of opportunity
ATM	atmospheric instrument suite
CBE	current best estimate
C&DH	command and data handling
CDR	critical design review
CFAS/	Swiss Federal Space Affairs Commission
CML	concept maturity level
CNES	Centre National d'Études Spatiales (French National Center of Space Research)
DGB	Disk-Gap-Band
DHMR	dry heat microbial reduction
DIMES	Descent Image Motion Estimating System
DLR	Deutsches Zentrum für Luft- und Raumfahrt e.V. (German Aerospace Center)
DOF	degrees of freedom
DOR	Differential One-way Ranging
DSN	Deep Space Network
DTE	direct to Earth
EDL	entry, descent, and landing
EM	electromagnetic
EMS	electromagnetic sounder
ESA	European Space Agency
FMI	Finnish Meteorological Institute
FY	fiscal year
GDS	ground data system
GEP	Geophysical and Environmental Package
HiRISE	High Resolution Imaging Science Experiment
HP^3	heat flow probe
IB	isothermal block
IDA	instrument deployment arm
IDC	instrument deployment camera
IMU	inertial measurement unit
IPGP	Institut de Physique du Globe de Paris
JPL	Jet Propulsion Laboratory
MEL	master equipment list
MEPAG	Mars Exploration Program Advisory Group
MER	Mars Exploration Rover
MEV	maximum expected value
MGN	Mars Geophysical Network
MLI	multilayer insulation
MOLA	Mars Orbiter Laser Altimeter
MOO	Mission of Opportunity
MOS	mission operations system
MPF	Mars Pathfinder
MPL	Mars Polar Lander
MT	magnetotelluric method
MRO	Mars Reconnaissance Orbiter
MVACS	Mars Volatiles and Climate Surveyor
NRC	National Research Council
PI	principal investigator
PLUTO	Planetary Underground Tool
PPO	Planetary Protection Officer
PRODEX	Programme de Développement d'Experiences scientifiques
PRT	platinum resistance thermometer
RCS	reaction control system
SDST	small deep space transponder
SEIS	seismometer
SLA	super lightweight ablator

SP	short period
TC	thermocouple
TCM	trajectory correction maneuver
TIRS	Transverse Impulse Rocket Systems
TPS	thermal protection system
TRL	technology readiness level
UHF	ultra-high frequency
VBB	very broad band
WEM	warm electronics module
WBS	work breakdown structure

Appendix B. References

[1] Frey, H. V., J. H. Roark, K. M. Shockey, E. L. Frey, and S. E. H. Sakimoto (2002), Ancient lowlands on Mars, *Geophys. Res. Lett.,* **29**, doi: 10.1029/2001GL013832.

[2] Stevenson, D. J. (2001), Mars' core and magnetism, *Nature*, **412**, 214–219.

[3] Breuer D., and Spohn T. (2003), Early plate tectonics versus single-plate tectonics on Mars: Evidence from magnetic field history and crust evolution, *J. Geophys. Res.*, **108**(E7), 8-1, CiteID: 5072, doi: 10.1029/2002JE001999.

[4] Breuer D., and Spohn T. (2006), Viscosity of the Martian mantle and its initial temperature: Constraints from crust formation history and the evolution of the magnetic field, *Planet. Space Sci.*, **54**(2), 153–169, 10.1016/j.pss.2005.08.008.

[5] Schumacher S., and Breuer D., 2006, Influence of a variable thermal conductivity on the thermochemical evolution of Mars, *J. Geophys. Res.*, **111**(E2), CiteID: E02006, doi: 10.1029/2005JE002429.

[6] Dehant, V., H. Lammer, Y. Kulikov, J. M. Grießmeier , D. Breuer, O. Verhoeven, Ö. Karatekin, T. Van Hoolst, O. Korablev and P. Lognonné (2007), Planetary Magnetic Dynamo Effect on Atmospheric Protection of Early Earth and Mars, in *Geology and Habitability of Terrestrial Planets*, eds. K. Fishbaugh, P. Lognonné, F. Raulin, D. Des Marais, O. Korablev, *Space Science Series of ISSI*, vol. **24**, reprinted from *Space Science Reviews*, Springer, Dordrecht, The Netherlands, Space Science Reviews, doi: 10.1007/s11214-007-9163-9, 279-300.

[7] Dehant, V., W. Folkner, E. Renotte, D. Orban, S. Asmar, G. Balmino, J.-P. Barriot, J. Benoist, R. Biancale, J. Biele, F. Budnik, S. Burger, O. de Viron, B. Häusler, Ö. Karatekin, S. Le Maistre, P. Lognonné, M. Menvielle, M. Mitrovic, M. Pätzold, A. Rivoldini, P. Rosenblatt, G. Schubert, T. Spohn, P. Tortora, T. Van Hoolst, O. Witasse, and M. Yseboodt (2009), Lander Radioscience for obtaining the rotation and orientation of Mars, *Planet. Space Sci.*, **57**, 1050-1067, doi: 10.1016/j.pss.2008.08.009.

[8] Breuer, D., D. A. Yuen, and T. Spohn (1997), Phase transitions in the Martian mantle: Implications for partially layered convection, *Earth Planet. Sci. Lett.*, **148**(3–4), 457–469, doi: 10.1016/S0012-821X(97)00049-6.

[9] Spohn, T., M. H. Acuña, D. Breuer, M. Golombek, R. Greeley, A. Halliday, E. Hauber, R. Jaumann, and F. Sohl (2001), Geophysical Constraints on the Evolution of Mars, *Space Sci. Rev.*, **96**(1/4), 231–262.

[10] Van Thienen, P., K. Benzerara, D. Breuer, C. Gillmann., S. Labrosse, P. Lognonné, and T. Spohn (2007), Water, Life, and Planetary Geodynamical Evolution, in *Treatise of Geophysics*, Elsevier, eds. T. Herring and J. Schubert, **129**(1–3), 167–203, doi: 10.1007/s11214-007-9149-7.

[11] Spohn, T., F. Sohl., and D. Breuer (1998), Mars, *Astron. Astrophys. Rev.*, **8**(3), 181–235.

[12] Goins, N. R., and A. R. Lazarewicz (1979), Martian seismicity, *Geophys. Res. Lett.* **6,** 368–370.

[13] Nakamura, Y., and D. L. Anderson (1979), Martian wind activity detected by a seismometer at Viking lander 2 site, *Geophys. Res. Lett.*, **6**, 499–502.

[14] Phillips, R. J. (1991), Expected rate of marsquakes, in *Scientific Rationale and Requirements for a Global Seismic Network on Mars*, *LPI Tech. Rept. 91-02*, Lunar and Planetary Inst., Houston. pp. 35-38.

[15] Golombek, M. P., W. B. Banerdt, K. L. Tanaka, and D. M. Tralli (1992), A prediction of Mars seismicity from surface faulting, *Science*, **258**, 979–981.

[16] Knapmeyer, M., J. Oberst, E. Hauber, M. Wählisch, C. Deuchler, and R. Wagner (2006), Implications of the martian surface fault distribution and lithospheric cooling for seismicity: a working model, *J. Geophys. Res*. **111**, E11006.

[17] Davis, P. M. (1993), Meteoroid impacts as seismic sources on Mars, *Icarus*, **105**, 469–478.

[18] Lognonné, P., and C. Johnson (2007), Planetary Seismology, in *Treatises in Geophysics*, G. Shubert, ed., sec. 10.04, Elsevier.

[19] Lognonné, P., J. Gagnepain-Beyneix, W. B. Banerdt, S. Cacho, J.-F. Karczewski, and M. Morand (1996), An ultra broad band seismometer on InterMarsnet, *Planet. Space Sci.* **44**, 1237–1249.

[20] Mocquet, A. (1999), A search for the minimum number of stations needed for seismic networking on Mars, *Planet. Space Sci.,* **47**, 397–409.

[21] Gudkova, T. V., and V. N. Zharkov (2004), Mars: interior structure and excitation of free oscillations, *Phys. Earth Planet. Int.,* **142**, 1–22.

[22] Sohl, F., and T. Spohn (1997), The interior structure of Mars: Implications from SNC meteoroids, *J. Geophys. Res*., **102**, 1613–1636.

[23] Shapiro, N. M., and M. Campillo (2004), Emergence of broadband Rayleigh waves from correlations of the ambient seismic noise, *Geophys. Res. Lett*., **31**, doi: 10.1029/2004GL019491.

[24] Cazenave, A., and G. Balmino (1981), Meteorological effects on the seasonal variations of the rotation of Mars, *Geophys. Res. Lett.*, **8**, 245–248.

[25] Chao, B. F., and D. P. Rubincam (1990), Variations of Mars gravitational field and rotation due to seasonal CO_2 exchange, *J. Geophys. Res*., **95**, 14755–14760.

[26] Folkner, W. M., C. F. Yoder, D. N. Yuan, E. M. Standish, and R. A. Preston (1997), Interior Structure and Seasonal Mass Redistribution of Mars from Radio Tracking of Mars Pathfinder, *Science*, **278**(5344), 1749–1751.

[27] Yoder, C. F., and E. M. Standish (1997), Martian moment of inertia from Viking lander range data, *J. Geophys. Res.*, **102** (E2), 4065–4080.

[28] Defraigne, P., O. de Viron, V. Dehant, T. Van Hoolst, and F. Hourdin (2000), Mars rotation variations induced by atmospheric CO_2 and winds, *J. Geophys. Res.,* **105**, E10, 24563–24570.

[29] Dehant V., O. de Viron, Ö. Karatekin, and T. Van Hoolst (2006), Excitation of Mars polar motion, *Astron. Astrophys*., **446**(1), doi: 10.1051/0004-6361:20053825, 345–355.

[30] Van den Acker, E., T. Van Hoolst, O. de Viron, P. Defraigne, V. Dehant, F. Forget, and F. Hourdin (2002), Influence of the winds and of the CO_2 mass exchange between the atmosphere and the polar ice caps on Mars' orientation parameters, *J. Geophys. Res.,* 10.1029/2000JE001539.

[31] Sanchez, B., R. Haberle, and J. Schaeffer (2004), Atmospheric rotational effects on Mars based on the NASA Ames general circulation model: Angular momentum approach, *J. Geophys. Res.*, **109**(E8), CiteID: E08005, doi: 10.1029/2004JE002254.

[32] Karatekin, Ö., J. Duron, P. Rosenblatt, V. Dehant, T. Van Hoolst, and J.-P. Barriot (2005), Martian Time-Variable Gravity and its Determination; Simulated Geodesy Experiments, *J. Geophys. Res.*, **110**(E6), CiteID: E06001, doi: 10.1029/2004JE002378.

[33] Karatekin, Ö., T. Van Hoolst, J. Tastet, O. de Viron, and V. Dehant (2006), The effects of seasonal mass redistribution and interior structure on Length-of-Day variations of Mars, *Adv. Space Res*., **38**(4), 561-828, doi: JASR-D-04-01301R1.

[34] Karatekin, Ö., V. Dehant, and T. Van Hoolst (2006), Martian global-scale CO_2 exchange from time-variable gravity measurements, *J. Geophys. Res*., **111**, CiteID: E06003, doi: 10.1029/2005JE002591.

[35] Zuber, M., F. Lemoine, D. Smith, A. Konopliv, S. Smrekar, and S. Asmar (2007), The Mars Reconnaissance Orbiter Radio Science Gravity Investigation, *J. Geophys. Res.*, **112**, Issue E5, CiteID E05S07, doi: 10.1029/2006JE002833.

[36] Schulze-Makuch, D., and L. N. Irwin (2008), *Life in the Universe – Expectations and Constraints*, 2nd edition, Springer.

[37] Sonett, C. (1982), Electromagnetic Induction in the Moon, *Rev. Geophys*., **20**(3), 411-455.

[38] Khurana, K. K., M. G. Kivelson, D. J. Stevenson, G. Schubert, C. T. Russell, R. J. Walker, and C. Polanskey (1998), Induced magnetic fields as evidence for subsurface oceans in Europa and Callisto, *Nature,* **395***,* 777–780.

[39] Hood, L., D. Mitchell, R. Lin, M. Acuña, and A. Binder (1999), Initial Measurements of the Lunar Induced Magnetic Dipole Moment Using Lunar Prospector Magnetometer Data, *Geophys. Res. Lett*., **26**(15), 2327–2330.

[40] Wait, J. R., (1970), *Electromagnetic Waves in Stratified Media*, Pergamon, New York.

[41] Grimm R. E. (2002), Low-frequency electromagnetic exploration for groundwater on Mars, *J. Geophys. Res.,* **107**(E2), 5006*,* doi: 10.1029/ 2001JE001504.

[42] Gough, D. I., and M. R. Ingham (1983), Interpretation methods for magnetometer arrays, *Rev. Geophys*., **21**, 805–827.

[43] Espley J. R., G. T. Delory, and P. A. Cloutier (2006), Initial observations of low-frequency magnetic fluctuations in the Martian ionosphere, *J. Geophys. Res*., **111**, E06S22, doi:10.1029/2005JE002587.

[44] Rafkin, S., et al. (2009), *The Value of Landed Meteorological Investigations on Mars: The Next Advance for Climate Science*, White Paper submitted Sept. 15, 2009 to the National Research Council's 2009 Planetary Decadal Survey.